Electronic Supplementary Material (ESI)

Table of Contents

20.	^{1}H NMR titration experiment in **L** with Zn^{2+} addition in DMSO-d_6.	Fig. S12
21.	Benesi-Hildebrand plot determining the binding constant of L with Zn^{2+}.	Fig. S13
22.	LOD determination for Zn^{2+} ion.	Fig. S14
23.	Some reports of coumarin derivative to Zn^{2+} ion sensitivity	Table S5
24.	pH dependency on Zn^{2+} ion sensitivity.	Fig. S15
25.	Interference study on Zn^{2+} ion sensitivity (M= different metal ions present in 3 eqv.)	Fig. S16
26.	(a) Fluorescence spectra of ligand, L in absence and presence of various metal cations in 9:1 (v/v) EtOH/H_2O (HEPES buffer, pH 7.4 (b) vial image in normal light under UV light, 365 nm.	Fig. S17
27.	LOD determination for Cu^{2+} ion.	Fig. S18
28.	Fluorescence spectra of in-situ generated [Zn(**L′**)OAc] complex on incremental addition of Cu^{2+} ion in 9:1 (v/v) EtOH/H_2O (HEPES buffer, pH 7.4), $\lambda_{ex.}$ 400 nm.	Fig. S19
29.	X- Band EPR spectra (a) gradual addition of [Zn(**L′**)OAc] complex to $CuCl_2$ solution in CH_3CN (b) isolated [Cu(**L′′**)Cl] complex in CH_3CN.	Fig. S20
30.	(a) Absorbance spectra of ligand, L in absence and presence of various metal cations in 9:1 (v/v) EtOH/H_2O (HEPES buffer, pH 7.4; inset: zooming image at higher wavelength. (b) vial image in normal light.	Fig. S21
31.	(a) Absorbance spectra of ligand, **L** in absence and presence of various metal cations in 9:1 (v/v) EtOH/H_2O (HEPES buffer, pH 7.4; inset: zooming image at higher wavelength. (b) vial image in normal light.	Fig. S22
32.	Cyclic voltammograms of **L** and **L** with addition of $CuCl_2$ in CH_3CN	Fig. S23
33.	Absorbance spectra of L+Cu^{2+} and L+Zn^{2+}+Cu^{2+}.	Fig. S24
34.	Job's plot for binding stoichiometry determination for [Zn(L′)OAc]	Fig. S25

Experimental section

Materials and methods

All the reagents of analytical grade were collected from the commercial suppliers and used without further purification. 2-benzoyl pyridine and o-Phenylenediamine were obtained from Sigma-Aldrich and used as received.N^1-(phenyl(pyridin-2-yl)methyl)benzene-1,2-diamine and 7-hydroxy-4-methyl-2-oxo-2H-chromene-8-carbaldehyde were synthesized by following reported procedure.[1,2] The other inorganic salts and organic chemicals were bought from TCI chemicals and Merck. For spectroscopic measurement solvents with spectroscopic grade were used. Before using the solvents for spectroscopic studies these were dried by standard procedures.[3]Milli-Q water (Millipore) was used for preparation of aqueous solutions of metal salts. Perkin-Elmer (2400 Series-II, Perkin Elmer, USA) CHN analyzerwere used for elemental analysis purpose. The spectra were recorded by Lambda 25 spectrophotometer: UV-Vis; LS55: fluorescence and LX-1FTIR spectrophotometer: FT-IR spectra (KBr disk, 4000-400 cm^{-1}) on Perkin Elmer instruments. ^1H and ^{13}C NMR spectra were taken by Bruker 500 MHz FT-NMR spectrometer (TMS, internal standard). ESI-MS spectra were obtained from HRMS spectrometer (model, XEVO-G2QTOF#YCA351). The X-band EPR spectra were taken by a Magnettech GmbH MiniScope MS400 spectrometer where the microwave frequency was measured with an FC400 frequency counter. The electro analytical instrument, BASi Epsilon-EC for cyclic voltammetric experiments in CH_3CN solutions containing 0.2 M tetrabutylammonium hexafluorophosphate as a supporting electrolyte was used. For the electrochemical measurements the BASi platinum working electrode, platinum auxiliary electrode, Ag/AgCl reference electrode were used. The redox potential data reported were referenced to Fc^+/Fc (ferrocenium/ferrocene) couple.

Calculation of Limit of Detection (LOD) and Quantum yield

The LOD (limit of detection) was calculated from the fluorescence titration experiment acquired by gradual addition of Zn^{2+} ion to the ligand (**L**) solution (for Zn^{2+}) and addition of Cu^{2+} ion to the $[Zn(\mathbf{L'})]^+$ complex solution (for Cu^{2+}). The standard deviation was determined from the emission intensity of the free ligand (for Zn^{2+}) and $[Zn(\mathbf{L'})]^+$ (for Cu^{2+}) with varying the concentration. The limit of detection for Zn^{2+} and Cu^{2+} were determined by following the equation: LOD = 3 σ/m where σ is standard deviation; m is the slope of the curve acquired by fluorescence titration experiment by gradual addition of selective metal ions.

Fluorescence quantum yields (Φ) were obtained by using the equation:

$\Phi_{sample} = (OD_{std.} \times A_{sample})/(OD_{sample} \times A_{std.}) \times \Phi_{std.}$

Where, A_{sample} and A_{std} represent the areas under the fluorescence spectral curves for sample and standard respectively. OD_{sample} and $OD_{std.}$are the optical densities of the sample and standard respectively at the excitation wavelength.[4] In this work, acidic quinine sulfate was taken as the standard with known quantum yield, $\Phi_{std.}$ = 0.54 for the quantum yield calculation of ligand **L** and $[Zn(\mathbf{L'})]^+$ complex.

Common solution preparation for UV-Vis and fluorescence measurements

The 1.0×10^{-3} M stock solution of ligand **L** was prepared in THF. All the required metal cation solution of 1.0×10^{-3} M was arranged in deionized water. 50 μM, **L** solution was prepared in 9:1 (v/v) EtOH/H_2O (HEPES buffer, pH 7.4). The sensitivity and selectivity and all the UV-Vis as well as fluorescence measurements towards metal cations were checked by taking the above stock solution and to this solution 1.0 equivalent metal salt used. Titration of the resulting complex, $[Zn(\mathbf{L'})]^+$ of 50 μM was carried out by gradual addition of Cu^{2+} ion (0-52 μM). The

absorption and emission path length of the cell used were 1 cm.Fluorescence experiments were carried out using a 10 nm × 5 nm slit width.

Cell line culture and cell imaging study

Hep G2 (Human liver cancer) and WI-38 (human lung fibroblast) cells were acquired from NCCS (National Center for Cell Science) Pune, India. The cells were grown in DMEM with 10% FBS (Fetal Bovine Serum), penicillin/streptomycin (100 units/ml) and 5% CO_2. The measurements were carried out at a cell density permitting exponential growth and at 37ºC. The Hep G2 cells were grown in coverslips for 24 h. The ligand solution was prepared by dissolving it in ethanol/water with at a ratio of 1:9 (v/v). Then the cells were either mock-treated or treated with 5 µM of ligand (**L**) and 10 µM Zn^{2+} salt in the presence or absence of 10 µM of Cu^{2+} and incubated for 24 h at 37ºC.[5] The cells were washed with 1×PBS. Then fluorescence microscope images are taken by mounting this on a glass slide and observed under Leica fluorescence microscope.

Cell survivability of the ligand, **L** was studied in WI-38 cell as reported ealier.[6] In briefly, cell viability of WI-38 cells after exposure to various concentrations of ligand was judged by MTT assay measurement. The cells were seeded in 96-well plates at 1×10^4 cells per well and exposed to ligand, **L** at varying concentration of 0 µM, 20 µM, 40 µM, 60 µM, 80 µM, 100 µM for 24 h. After incubation cells were washed with 1×PBS in twice and incubated with MTT solution (450 µg/ml) for 3-4 h at 37ºC. The above resulting formazan crystals were dissolved in an MTT solubilization buffer and the absorbance was measured at 570 nm on a spectrophotometer (BioTek) and the value was compared with control cells.

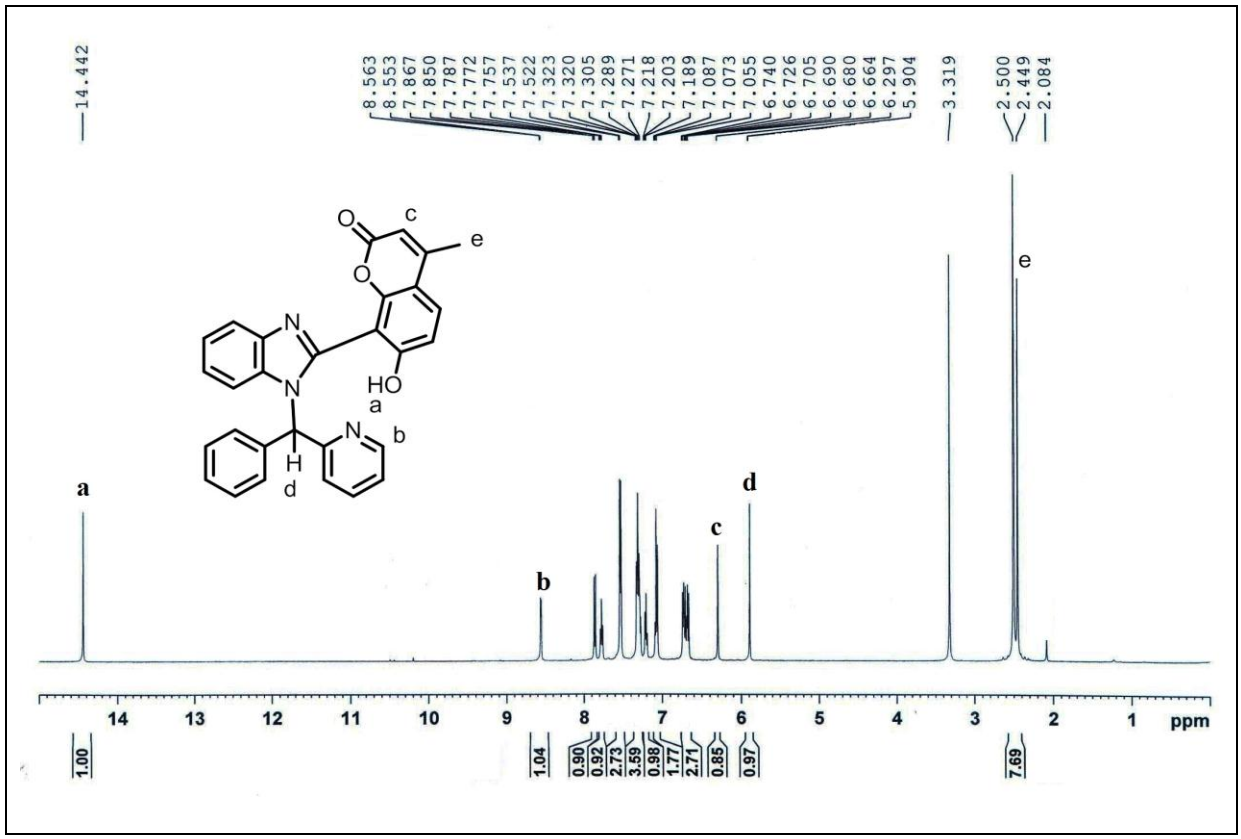

Fig. S1 ^{1}H NMR spectrum of **L** in DMSO-d_6.

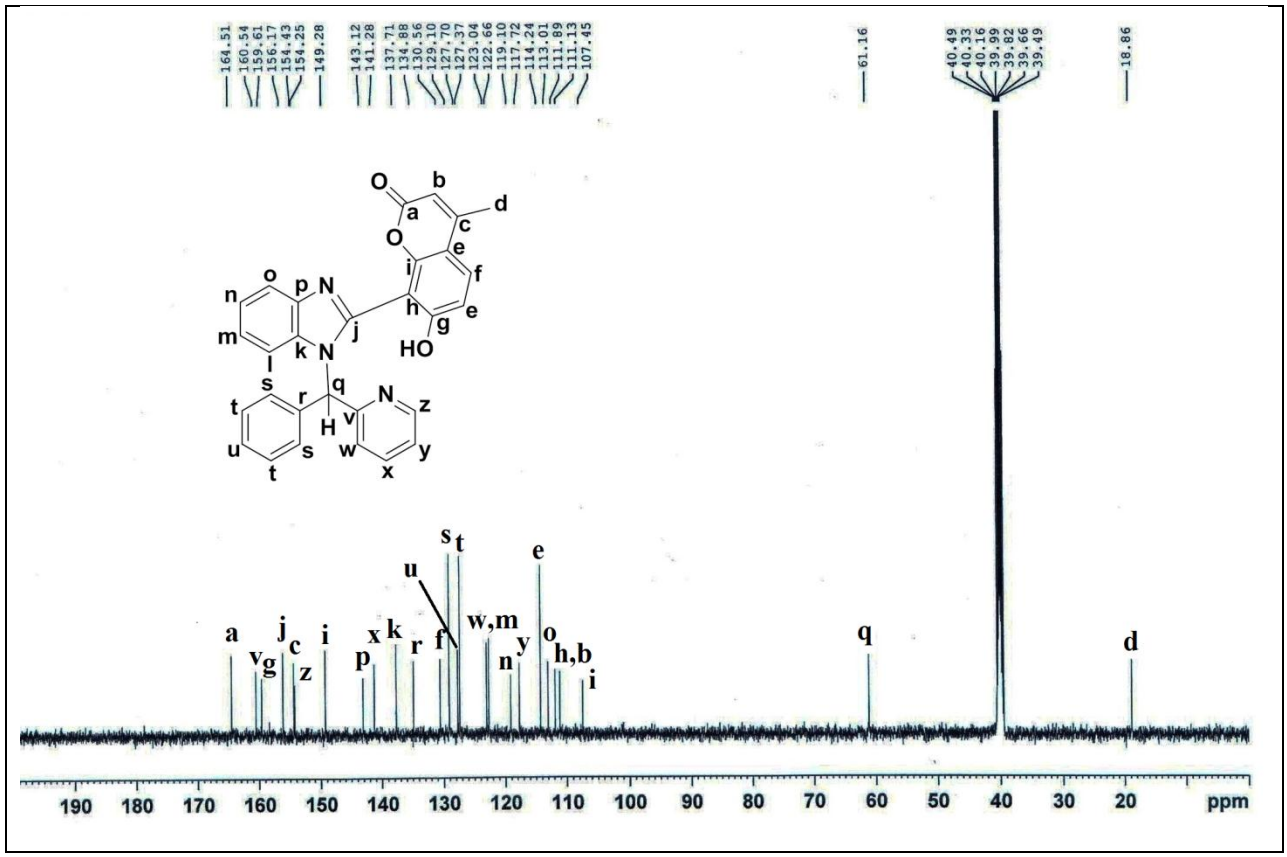

Fig. S2 ^{13}C NMR spectrum of **L** in DMSO-d_6.

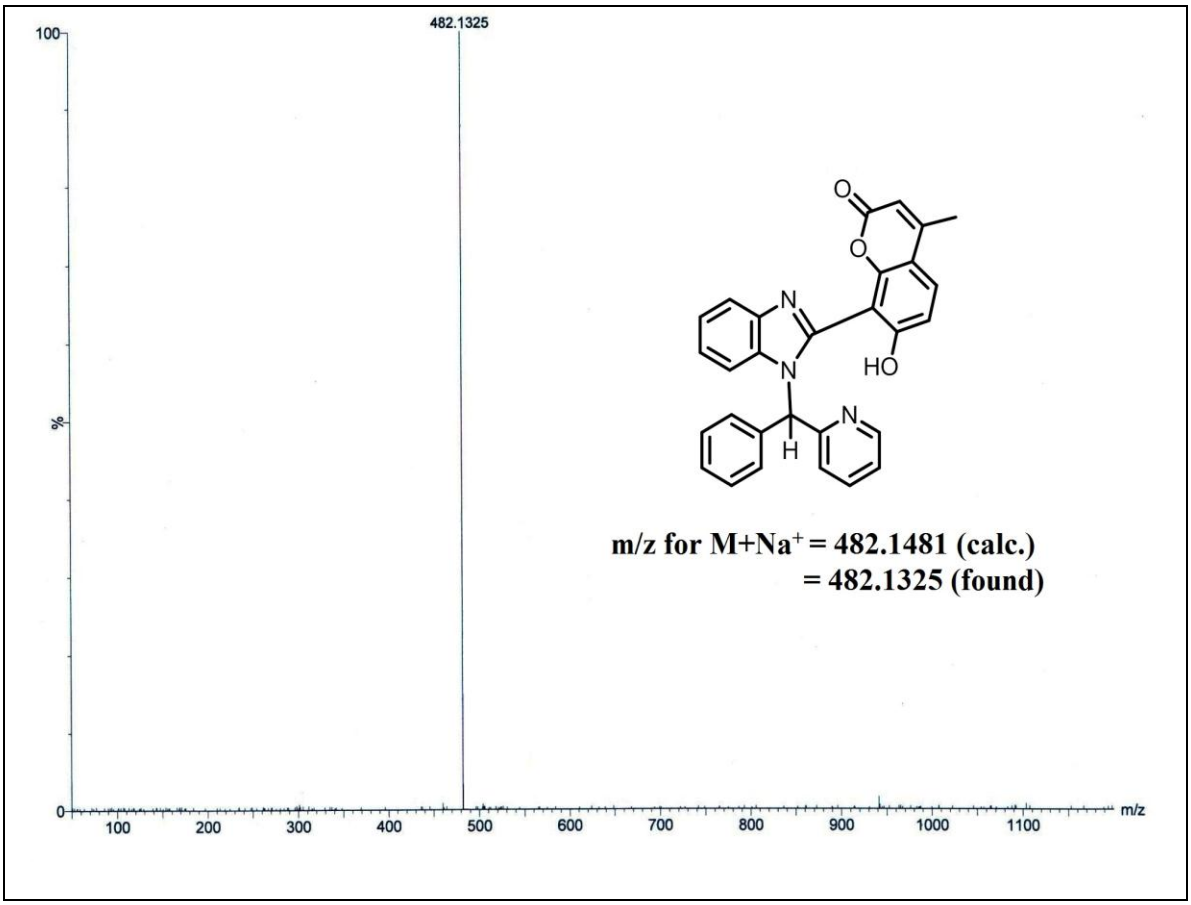

Fig. S3 ESI- MS spectrum of **L**.

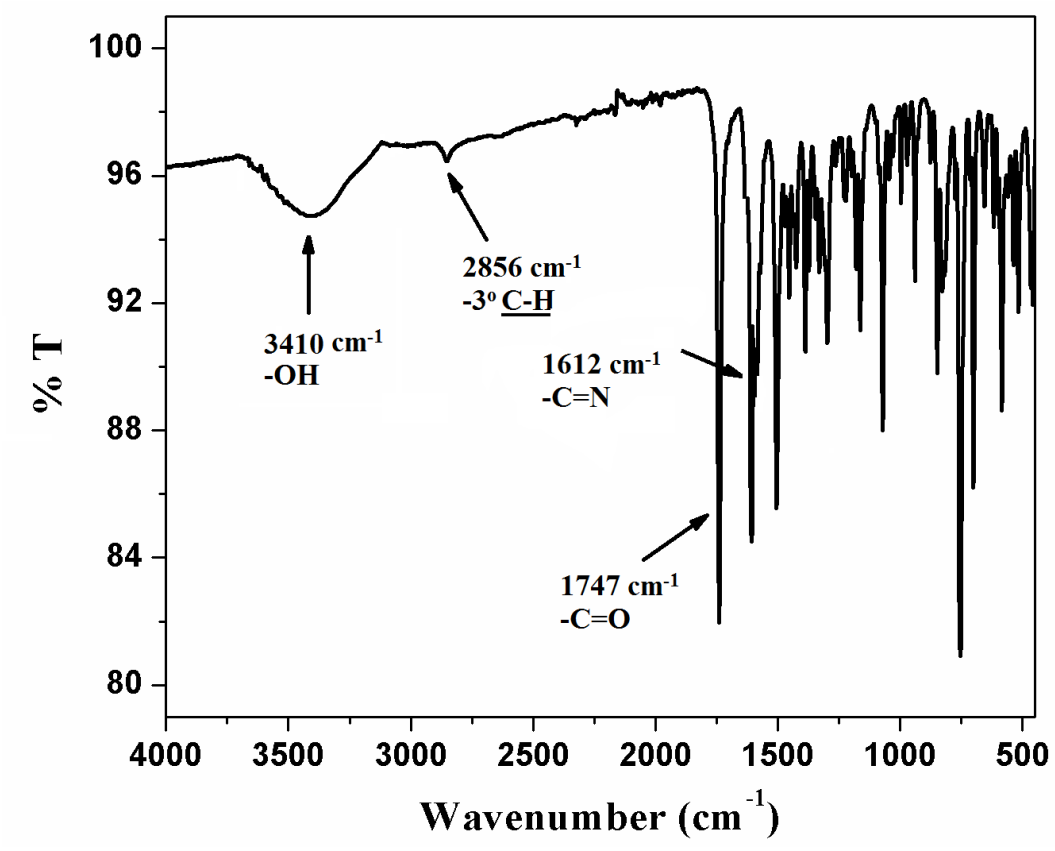

Fig. S4 FT-IR Spectrum of **L**.

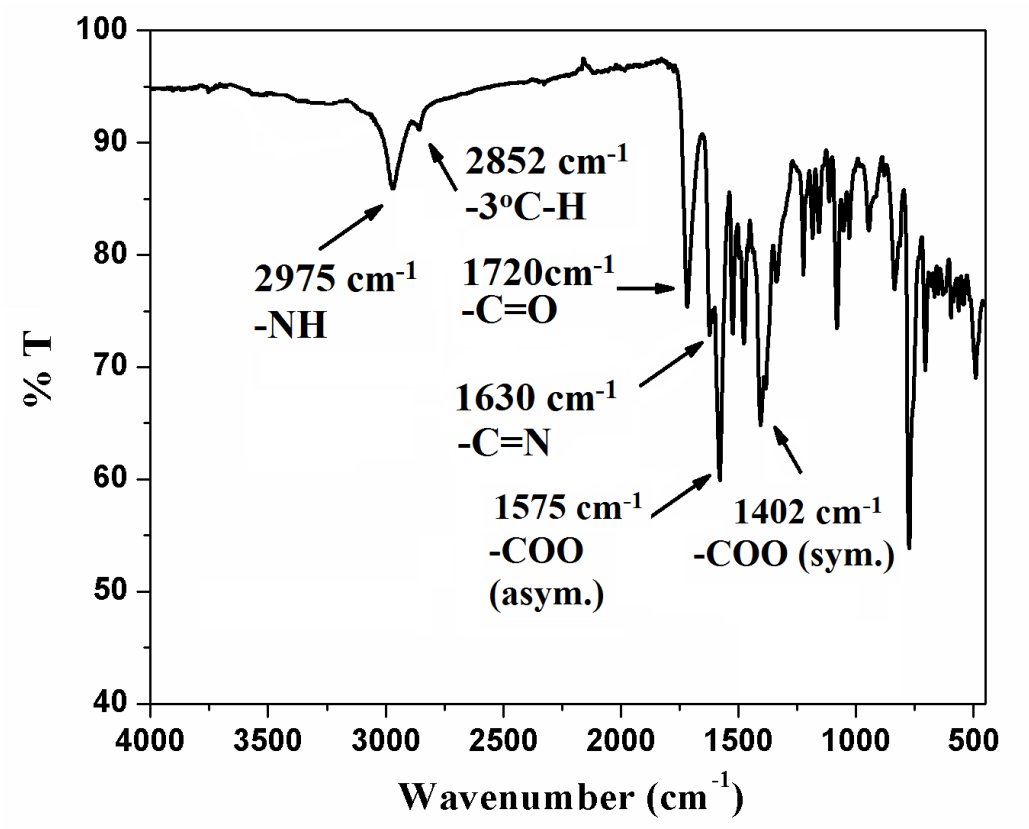

Fig. S5 FT-IR spectrum of [Zn(**L′**)OAc] complex.

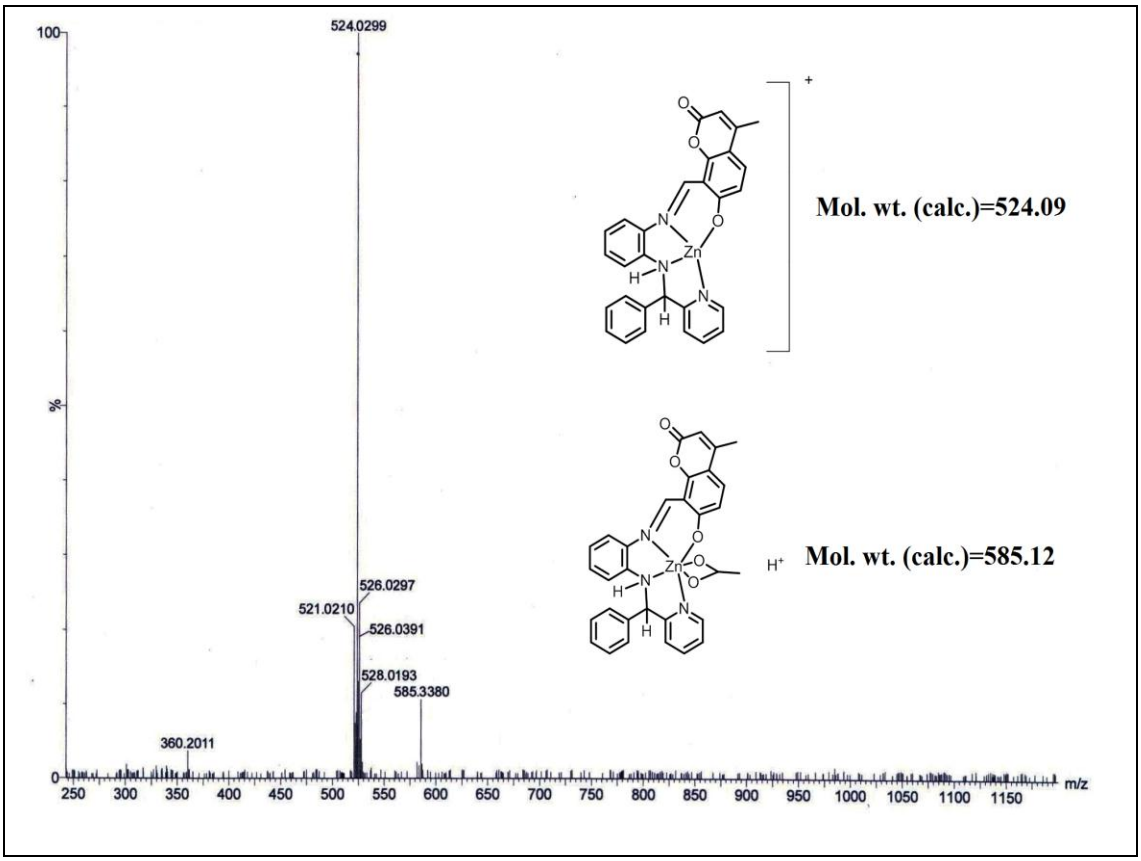

Fig. S6 ESI-MS spectrum of [Zn(**L′**)OAc] complex.

Table S1 Crystal data and refinement parameters for ligand, **L**, [Cu(**L″**)Cl] and [Cu(**L″**)ClO_4]

	L	[Cu(**L″**)Cl]	[Cu(**L″**)ClO_4]
Formula	$C_{29}H_{21}N_3O_3$	$C_{33}H_{28}C_{l3}Cu_2N_3O_4$	$C_{29}H_{20}ClCuN_3O_7$
fw	459.49	764.03	621.47
Crystal System	monoclinic	monoclinic	monoclinic
Space group	P 21/c	C 2/c	P 21/n
a (Å)	9.5747(9)	27.634(3)	11.799(2)
b (Å)	16.6202(15)	9.5387(9)	15.054(2)
c (Å)	14.3006(13)	27.062(3)	14.475(2)
α/°	90	90	90
β/°	90.226(3)	114.715(3)	90.113(5)
γ/°	90	90	90
V $(Å)^3$	2275.7(4)	6479.9(11)	2571.2(7)
Z	4	8	4
Dc/g cm^{-3}	1.341	1.566	1.605
μ/mm^{-1}	0.088	1.602	1.010
λ(Å)	0.71073	0.71073	0.71073
data[I >2σ(I)]/params	5033/318	5703/407	4505/ 371
GOF[c]	1.078	1.054	1.080
final R indices [I >2σ(I)][a,b]	R1 = 0.0744 wR2 = 0.1458	R1 = 0.0766 wR2 = 0.2502	R1 = 0.1151 wR2 = 0.2463

[a]$R_1 = \Sigma||F_o|-|F_c||/\Sigma|F_o|$; [b]$wR_2 = \{\Sigma[w(F_o^2-F_c^2)^2]/\Sigma[w(F^2_o)^2]\}^{1/2}$; $w = [\sigma^2(F_o)^2 + (0.1003P)^2 + 4.9693P]^{-1}(F_o^2 + 2F_c^2)/3$; [c] Goodness-of-fit

Table S2 Some important bond length and bond angles of **L**

Bond	**Length/Angle (Å/°)**	**Bond**	**Angle (°)**
O(1) - C(1)	1.353(3)	C(10) - N(2) - C(18)	125.9(2)
N(1) -C(10)	1.317(4)	O(1) - C(1) - C(2)	121.7(3)
N(2) - C(18)	1.472(4)	C(1) - C(2) - C(3)	120.7(3)
C(1) - C(9)	1.391(4)	C(1) - C(9) - C(8)	117.7(3)
C(18) - C(23)	1.527(4)	N(1) - C(10) - N(2)	113.0(2)
C(24) - C(29)	1.364(4)	N(1) - C(12) - C(13)	129.7(3)
N(4) - C(26)	1.342(5)	C(18) - C(23) - C(30)	120.7(3)
C(1) - C(2)	1.389(4)	N(4) - C(24) - C(29)	121.6(3)
N(2) - C(17)	1.389(3)	C(1) - O(1) - H(1)	109
C(18) - H(18)	0.98	N(2) - C(18) - H(18)	106
O(1) - H(1)	0.82	C(10) - N(1) - C(12)	104.9(2)
N(1) - C(12)	1.403(4)	O(1) - C(1) - C(9)	118.3(3)
N(4) - C(24)	1.338(4)	C(1) - C(9) - C(10)	122.1(3)
C(9) > C(10)	1.478(4)	N(1) - C(10) - C(9)	124.3(3)
C(18) - C(24)	1.516(4)	N(1) - C(12) - C(17)	109.8(2)
N(2) - C(10)	1.371(3)	N(2) - C(17) - C(12)	105.8(2)
C(20) - C(19) - C(30)	120.5(3)	N(2) - C(18) - C(23)	111.3(2)
C(18) - C(24) - C(29)	121.5(3)	C(1) - C(2) - H(2)	120
C(10) - N(2) - C(17)	106.5(2)	C(24) - N(4) - C(26)	117.4(3)

N(2) - C(10) - C(9)	122.7(2)	N(2) - C(17) - C(16)	132.3(3)
N(2) - C(18) - C(24)	110.4(2)	C(18) - C(23) - C(22)	120.7(3)
N(4) - C(24) - C(18)	116.9(3)	N(4) - C(26) - C(27)	124.6(4)
C(24) - C(18) - H(18)	106	N(4) - C(26) - H(26)	118
C(24) - C(29) - H(29)	121		

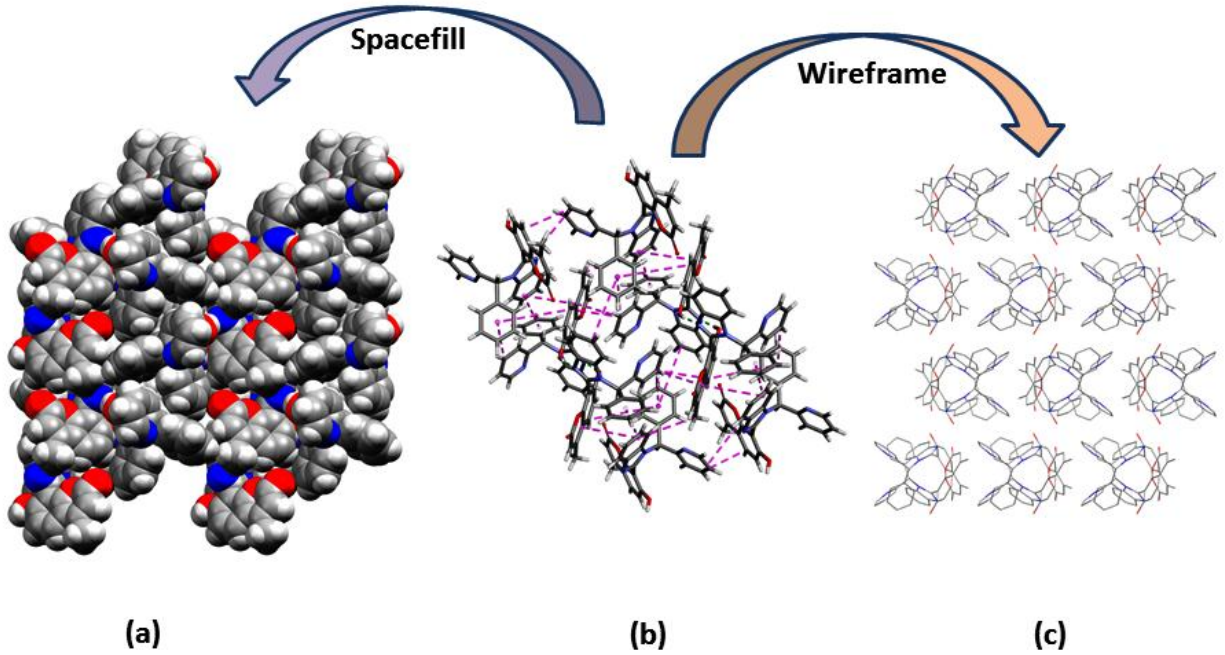

Fig. S7 (a) spacefill view of supramolecular aggregated ligand, **L** along crystallographic axis 'c' (b) different supramolecular interactions presents in **L** (c) supramolecular assembly of **L** along 'c' crystallographic axis showing 'bee' like molecular arrangement.

Table S3 Selected bond length and bond angles of [Cu(L″)Cl] complex

Bond	**Length/Angle (Å/°)**	**Bond**	**Angle (°)**
Cu(1) - Cl(1)	3.155(3)	Cl(2) - Cu(1) - N(1)	94.8(2)
Cu(1) - N(2)	1.954(7)	O(2) - Cu(1) - N(1)	97.2(2)
O(2) - C(1)	1.299(10)	N(1) - Cu(1) - N(2)	81.9(2)
N(1) - C(25)	1.356(9)	C(11) - N(3) - C(12)	122.9(6)
N(3) - C(11)	1.282(10)	N(3) - C(12) - C(17)	116.4(6)
C(10) - C(11)	1.433(10)	N(2) - C(17) - C(12)	112.6(6)
C(18) > C(25)	1.476(12)	N(2) - C(18) - C(19)	126.8(8)
Cu(1) - Cl(2)	2.556(7)	C(18) - C(19) - C(20)	118.7(7)
Cu(1) - N(3)	1.931(6)	N(1) - C(25) - C(26)	120.8(8)
N(1) - C(29)	1.347(10)	C(1) - C(2) - H(2)	119
N(3) - C(12)	1.424(9)	N(3) - C(11) - H(11)	118
C(12) - C(13)	1.386(11)	C(1) - C(10) - C(9)	117.1(7)
Cu(1) - O(2)	1.879(5)	N(3) - C(11) - C(10)	124.9(8)
Cu(2) - Cl(1)	2.108(4)	N(2) - C(17) - C(16)	126.9(7)
N(2) - C(17)	1.447(11)	N(2) - C(18) - C(25)	113.6(7)
C(1) - C(2)	1.417(10)	C(18) - C(19) - C(24)	121.6(7)
C(12) - C(17)	1.417(10)	C(18) - C(25) - C(26)	123.7(7)
C(11) - H(11)	0.93	C(10) - C(11) - H(11)	118
Cu(1) - N(1)	1.979(6)	C(1) - C(10) - C(11)	124.8(7)
N(2) - C(18)	1.293(11)	N(3) - C(12) - C(13)	124.8(6)
C(1) - C(10)	1.421(11)	C(12) - C(13) - C(14)	120.0(8)
C(18) > C(19)	1.491(11)	C(12) - C(17) - C(16)	120.5(8)
C(25) - C(26)	1.366(13)	N(1) - C(25) - C(18)	115.5(7)
N(1) - C(29) - C(28)	122.1(7)	C(25) - C(26) - C(27)	119.3(8)
C(12) - C(13) - H(13)	120	C(25) - C(26) - H(26)	120
N(1) - C(29) - H(29)	119		

Table S4 Selected bond length and bond angles of [Cu(L″)(ClO_4] complex

Bond	Length/Angle (Å/°)	Bond	Length/Angle (Å/°)
Cu(1) - O(1)	1.855(6)	O(1) - Cu(1) - O(5)	94.0(4)
Cu(1) - N(3)	1.915(7)	O(1) - Cu(1) - N(3)	97.2(3)
N(2) - C(18)	1.322(12)	N(2) - Cu(1) - N(3)	84.0(3)
C(18) > C(19)	1.472(15)	Cu(1) - O(5) - Cl(1)	142.3(8)
O(1) - C(1)	1.309(11)	C(7) - N(3) - C(12)	124.0(8)
N(1) - C(19)	1.340(13)	N(3) - C(7) - C(6)	126.2(8)
N(3) - C(7)	1.304(12)	N(3) - C(12) - C(17)	116.4(9)
C(18) > C(24)	1.465(15)	N(2) - C(17) - C(12)	112.2(9)
Cu(1) - N(1)	1.977(7)	N(2) - C(18) - C(19)	111.8(9)
N(1) - C(23)	1.314(13)	N(1) - C(19) - C(18)	117.1(9)
N(3) - C(12)	1.396(13)	N(1) - C(23) - C(22)	120.3(9)
Cu(1) - N(2)	1.925(8)	O(1) - Cu(1) - N(1)	96.2(3)
N(2) - C(17)	1.417(13)	N(1) - Cu(1) - N(2)	82.5(3)
Cu(1) - O(1) - C(1)	126.6(6)	Cu(1) - N(1) - C(19)	111.0(6)
Cu(1) - N(2) - C(17)	114.3(6)	Cu(1) - N(3) - C(7)	123.0(6)
O(1) - C(1) - C(2)	118.7(8)	N(2) - C(17) - C(16)	126.7(9)
N(2) - C(18) - C(24)	127.6(9)	N(1) - C(19) - C(20)	119.6(9)
N(3) - C(7) - H(7)	117	N(1) - C(23) - H(23)	120
O(1) - Cu(1) - N(2)	178.1(3)	N(1) - Cu(1) - N(3)	165.9(3)
Cu(1) - N(1) - C(23)	126.4(7)	Cu(1) - N(2) - C(18)	116.2(7)
Cu(1) - N(3) - C(12)	113.1(6)	O(1) - C(1) - C(6)	122.1(9)

C(18) - C(19) - C(20)	123.3(9)	C(18) - C(24) - C(29)	120.8(10)

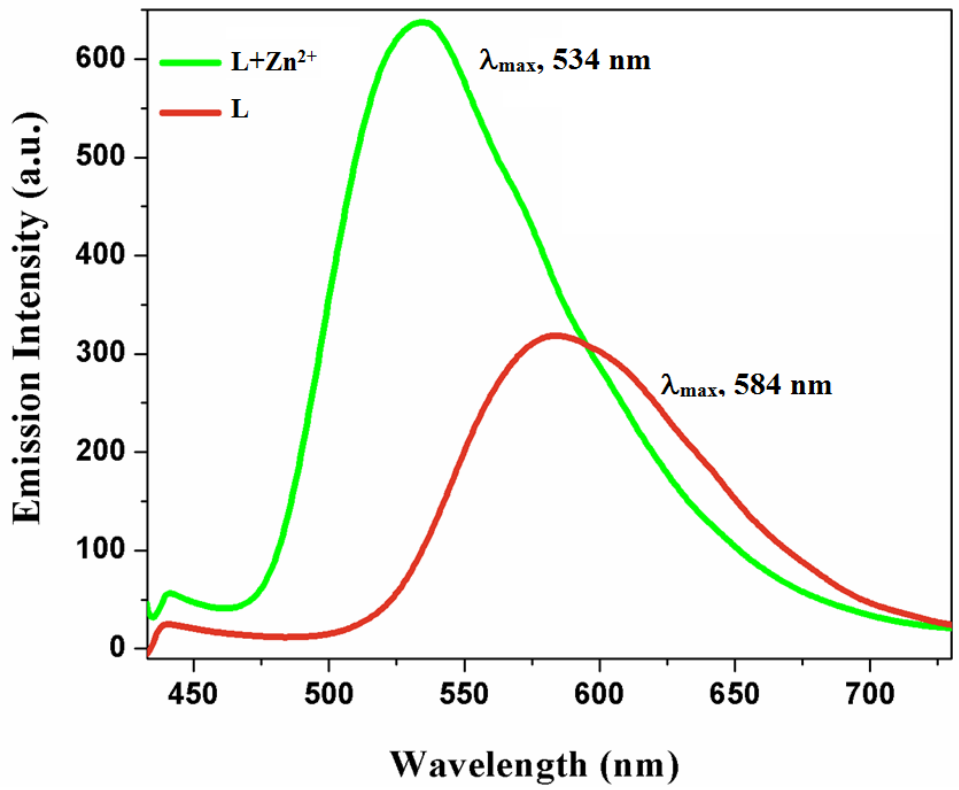

Fig. S8 Solid state emission spectrum of the ligand, **L** and **L**-Zn^{2+}complex (λ_{ex} 400 nm, excitation slit 15 nm and emission slit 5 nm).

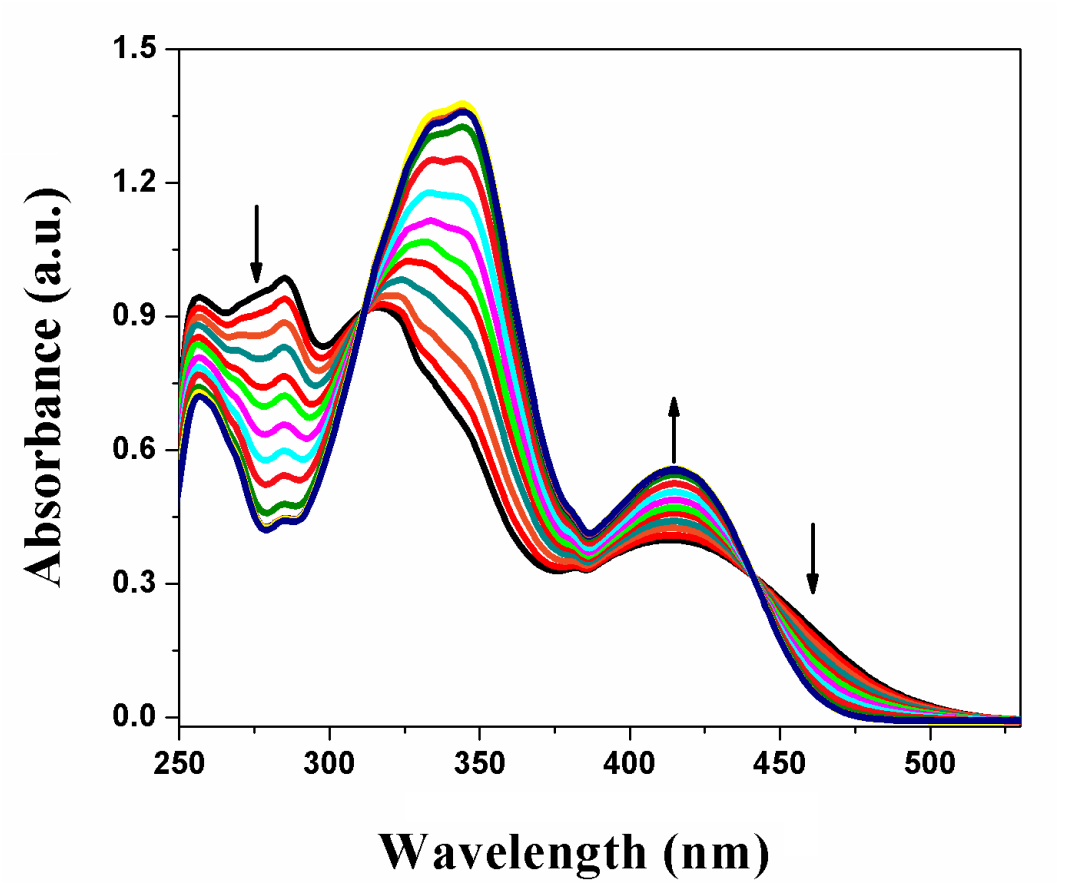

Fig. S9 Absorbance spectral change of ligand, **L** on incremental addition of Zn^{2+} ion in 9:1 (v/v) EtOH/H_2O (HEPES buffer, pH 7.4).

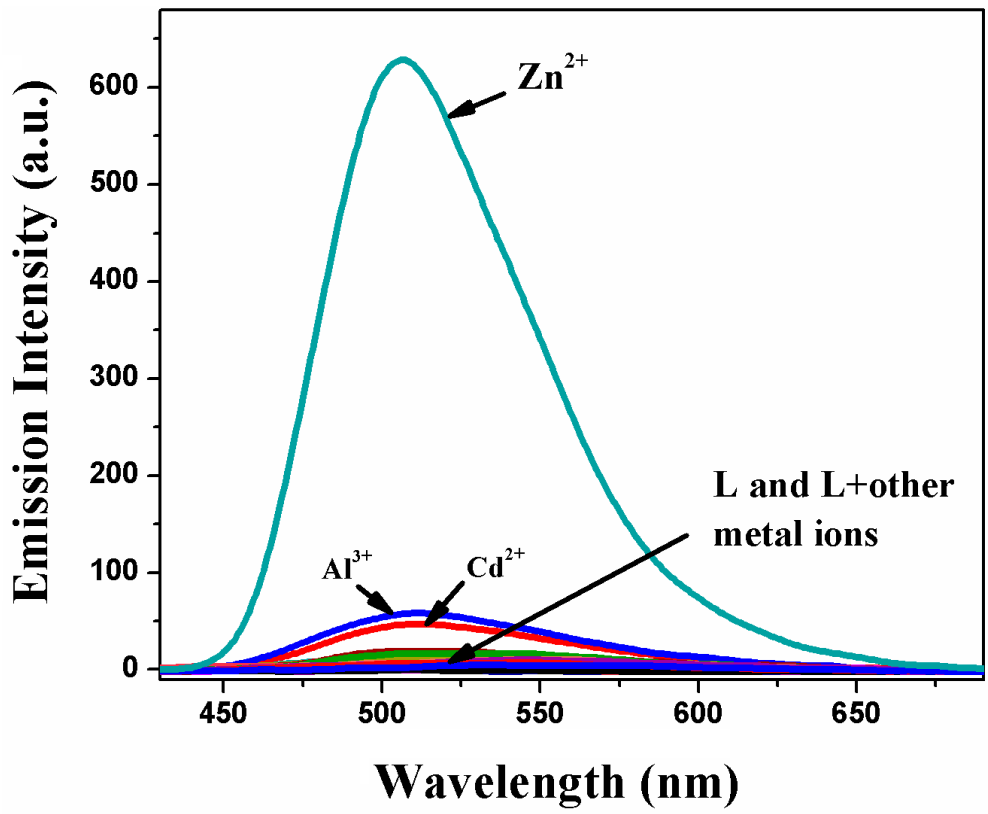

Fig. S10 Fluorescence spectra of ligand, **L** in presence of various cations in 9:1 (v/v) EtOH/H_2O (HEPES buffer, pH 7.4), $\lambda_{ex.}$ 400 nm.

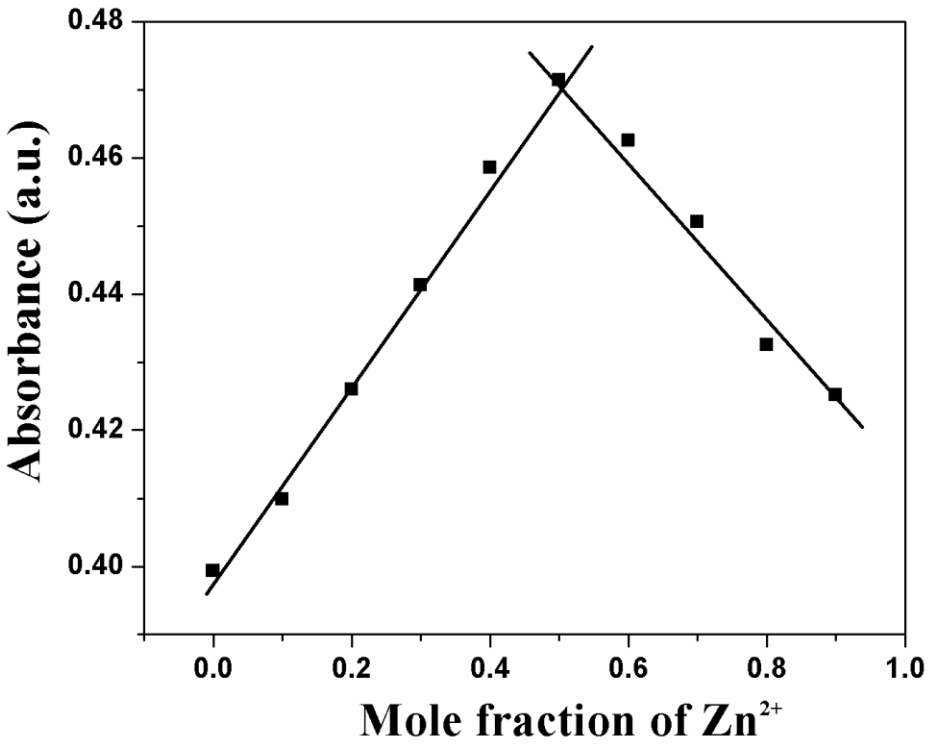

Fig. S11 Job's plot for binding stoichiometry determination in **L** with Zn^{2+}.

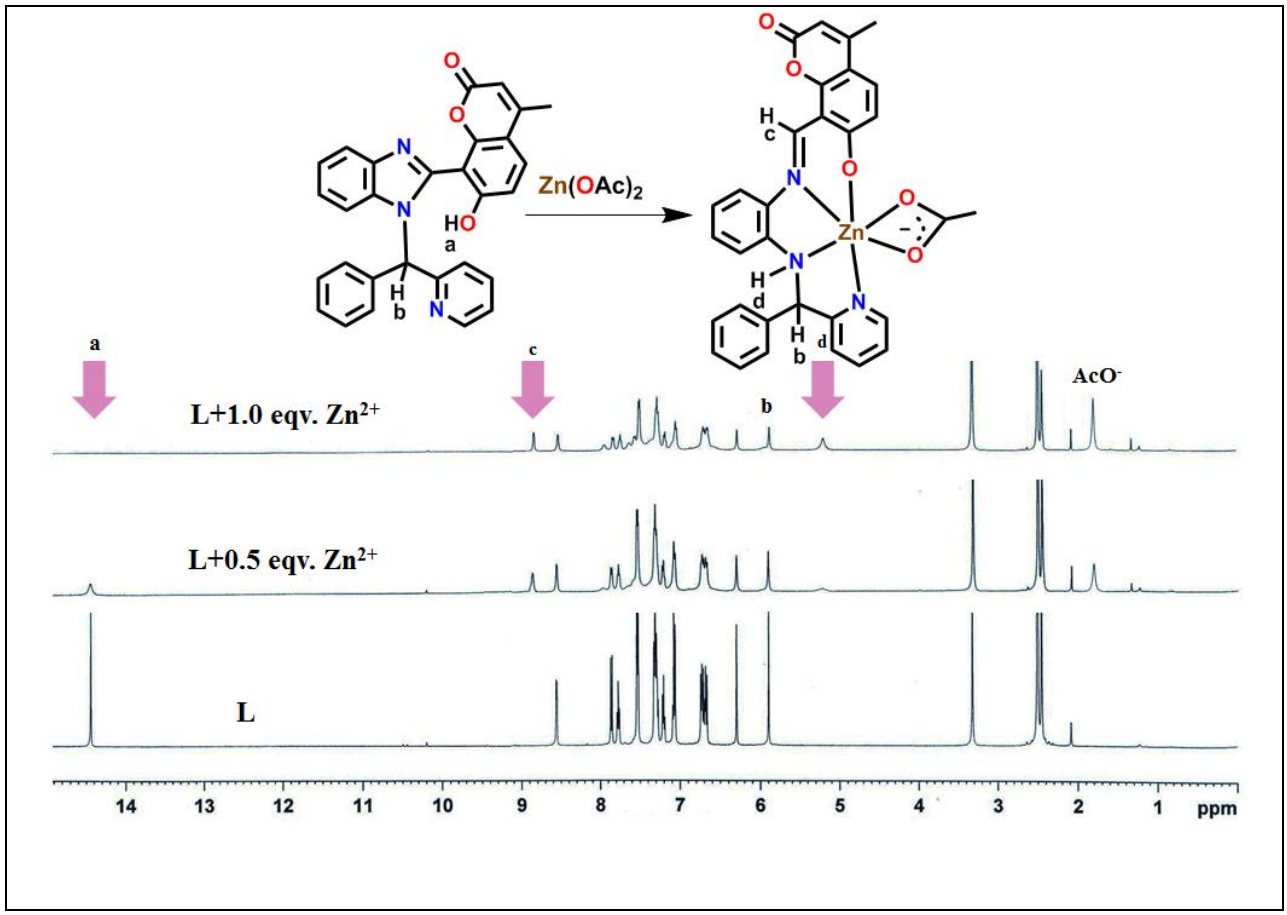

Fig. S12 ^{1}H NMR titration experiment in **L** with Zn^{2+} addition in DMSO-d_6.

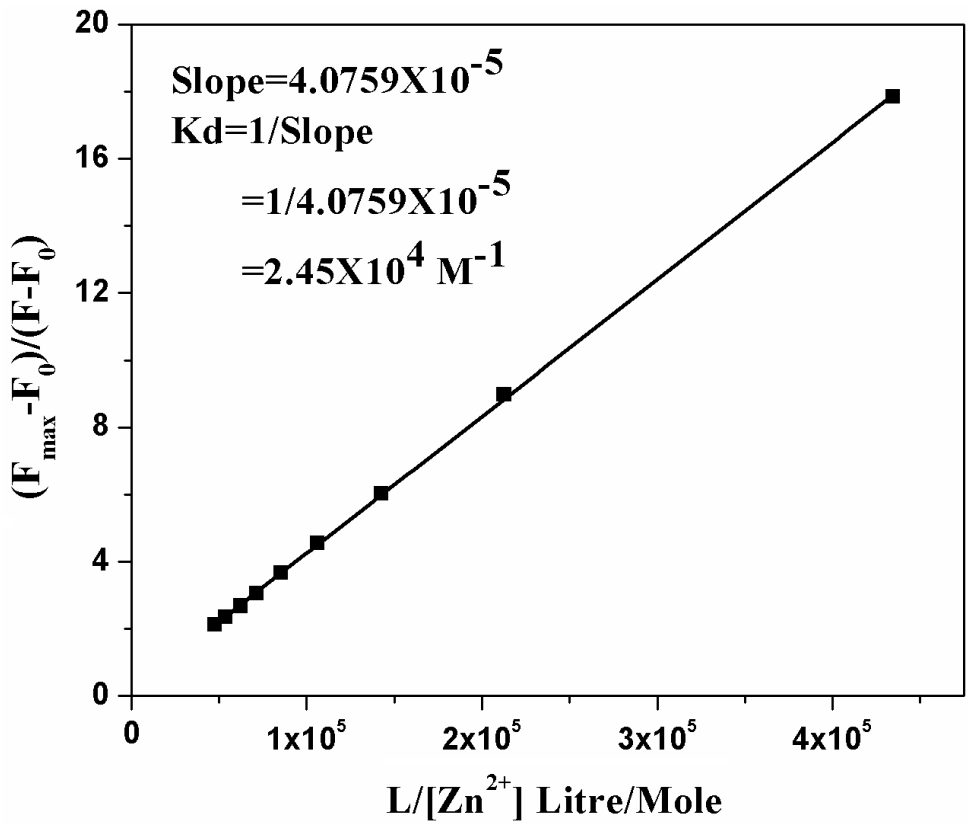

Fig. S13 Benesi-Hildebrand plot determining the binding constant of **L** with Zn^{2+}.

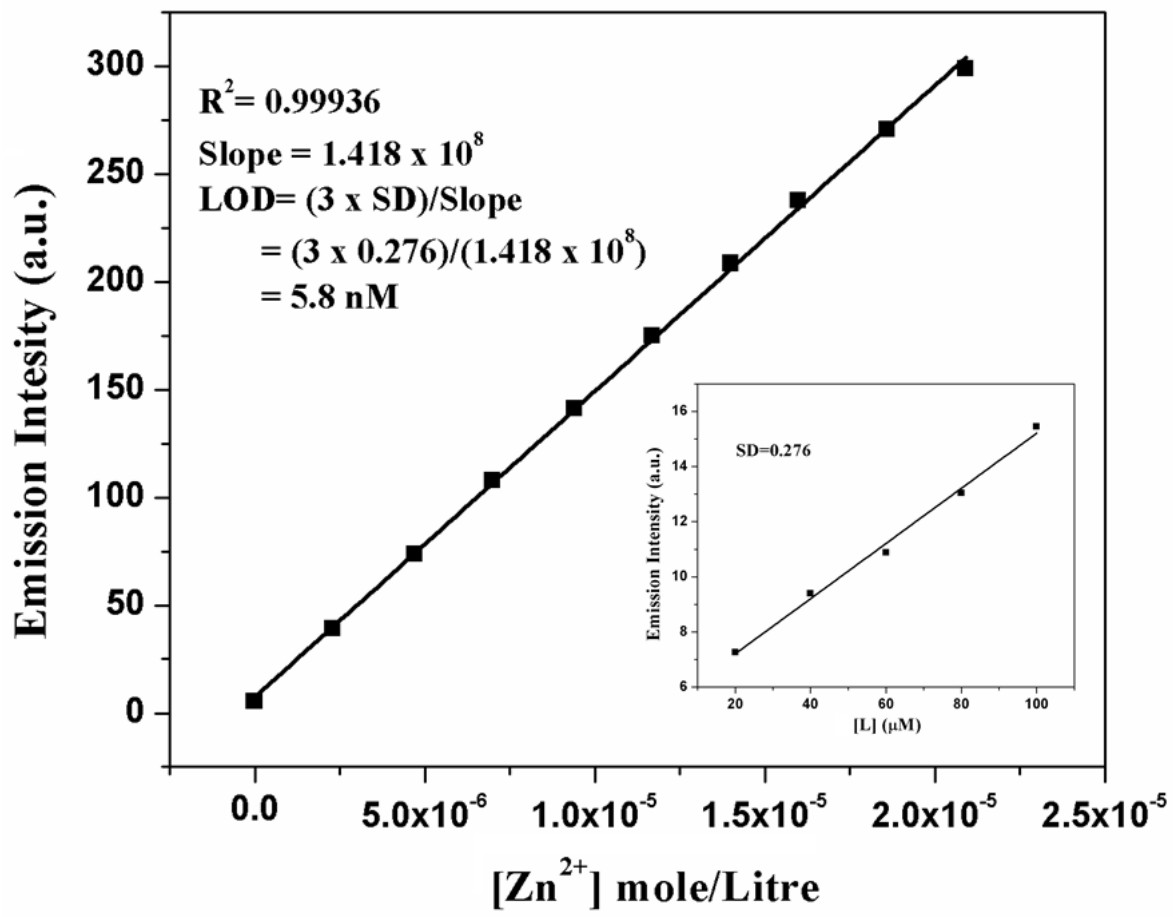

Fig. S14 LOD determination for Zn^{2+} ion.

Table S5 Some reports of coumarin derivative to ion sensitivity

Sl. No.	Ligand	Selectivity (LOD)	Solvent	Solid state sensing Study	Live cell imaging	Ref.
1.	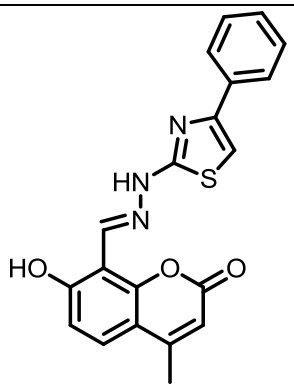	Zn^{2+} (72 nM) and AcO^- (94 nM)	DMSO/H_2O (v/v = 3:7)pH, 7.2	No	Yes	[7]

2.	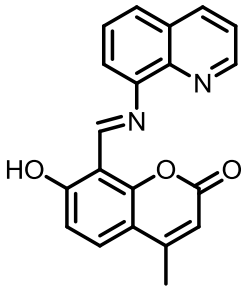	Zn^{2+} (100 nM)	THF	Yes	No	[8]
3.	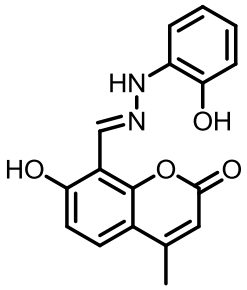	CN^- (169 nM) And Zn^{2+} (61 nM)	DMSO/H_2O 3:7, v/v	Yes	No	[9]
4.	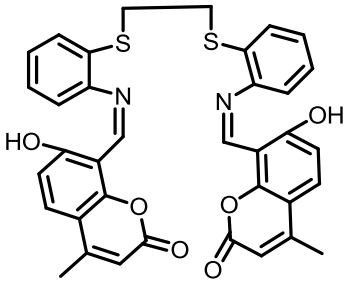	Zn^{2+} (68 nM) and ATP (6.7 μM)	MeOH/H_2O (v/v, 2 : 1)	No	Yes	[10]
5.	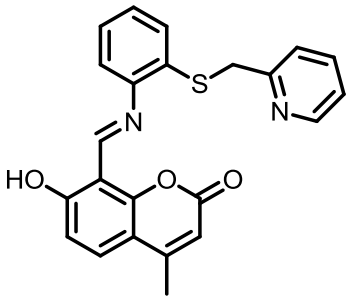	Zn^{2+} (78 nM) and ATP (6.6 μM)	MeOH/H_2O (v/v, 3:1)	No	Yes	[11]
6.	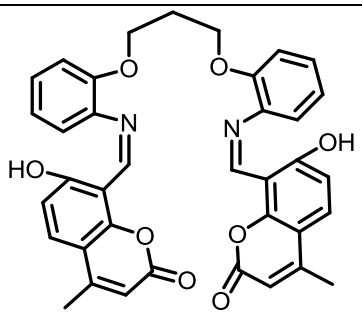	Zn^{2+} (11 nM)	9 : 1 v/v CH_3CN : H_2O	Yes	Yes	[12]

7.	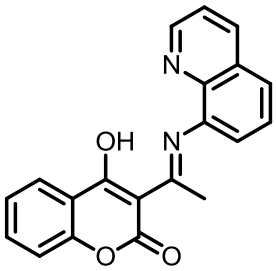	Zn^{2+} (-)	CH_3CN/H_2O mixture (1:1, v/v)	No	No	[13]
8.	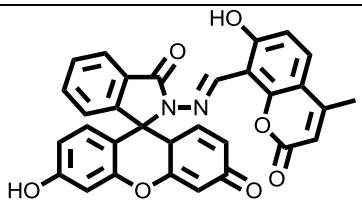	Zn^{2+} (100 nM)	EPES buffer of PH 7.4	No	No	[14]
9.	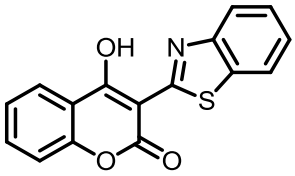	Zn^{2+} (35 nM)	CH_3CN/H_2O (95:5, v/v)	No	Yes	[15]
10.	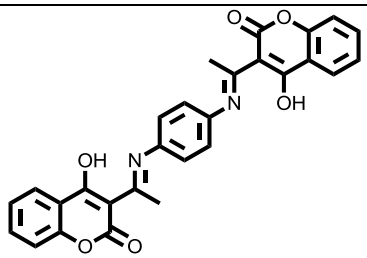	Zn^{2+} (19 nM) and Cu^{2+} (1.87 nM)	CH_3CN : H_2O (1 : 1, v/v, pH, 7.2)	No	No	[16]
11.	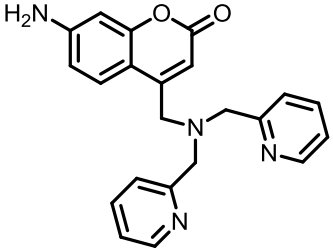	Zn^{2+} (26 nM) and ClO^- (2 μM)	10 mM HEPES buffer (pH 7.4)	No	No	[17]
12.	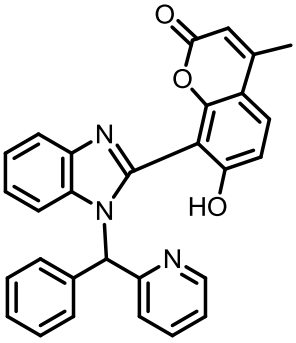	Zn^{2+} (5.8 nM) and Cu^{2+} (20 nM)	9:1, v/v $EtOH/H_2O$	Yes	Yes	This work

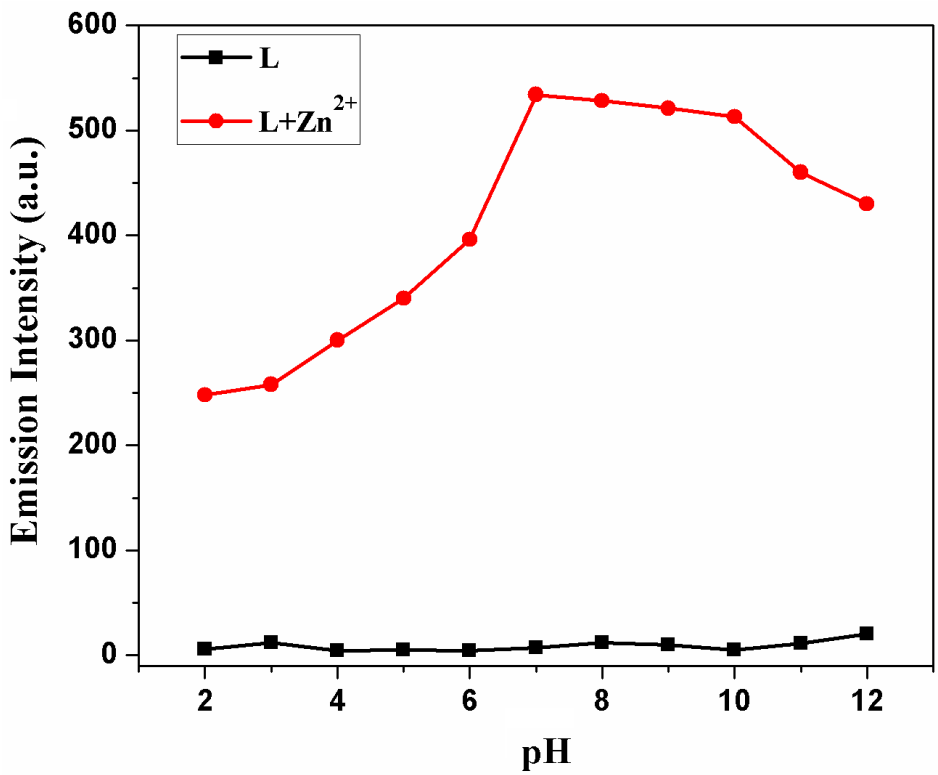

Fig. S15 pH dependency on Zn^{2+} ion sensitivity.

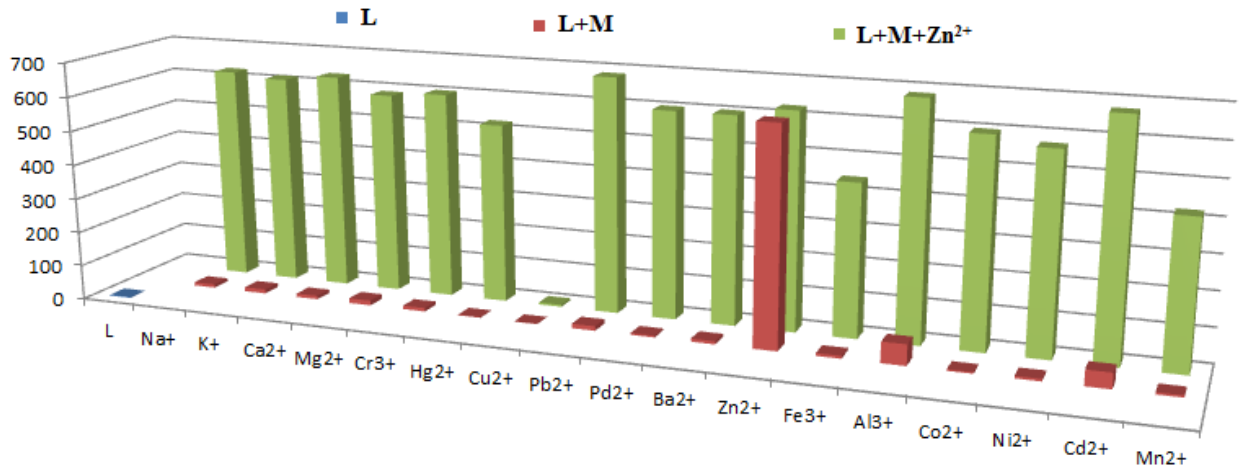

Fig. S16 Interference study on Zn^{2+} ion sensitivity (M= different metal ions present in 3 eqv.)

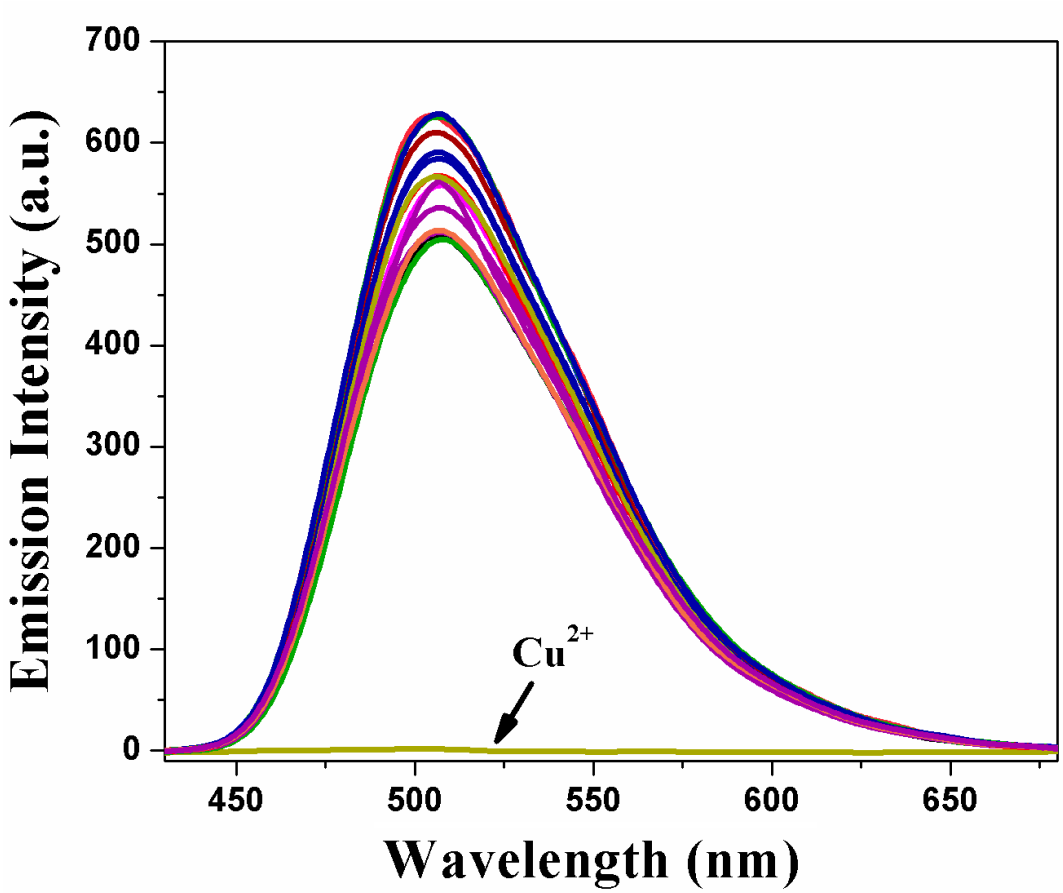

(a)

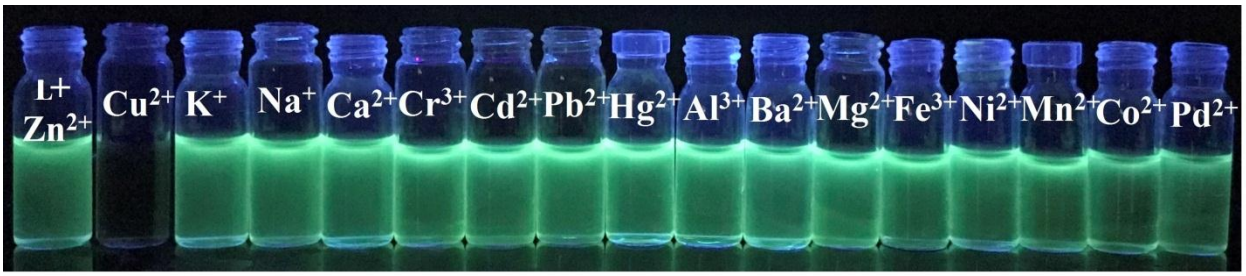

(b)

Fig. S17 (a) Fluorescence spectra of ligand, **L** in absence and presence of various metal cations in 9:1 (v/v) EtOH/H_2O (HEPES buffer, pH 7.4 (b) vial image in normal light under UV light, 365 nm.

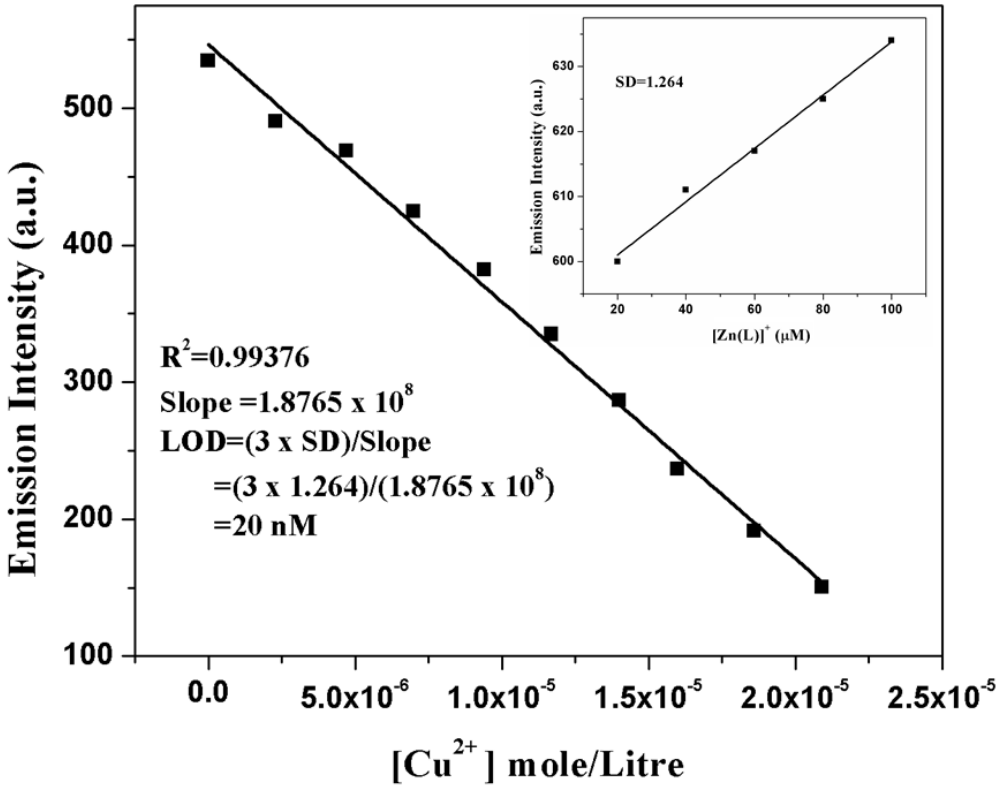

Fig. S18 LOD determination for Cu^{2+} ion.

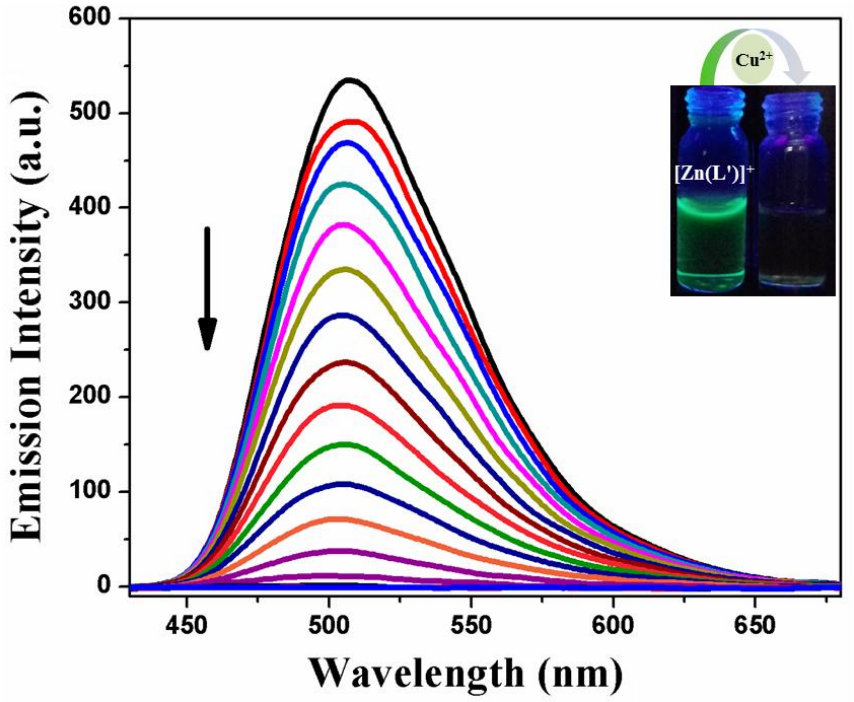

Fig. S19 Fluorescence spectra of in-situ generated [Zn(**L′**)OAc] complex on incremental addition of Cu^{2+} ion in 9:1 (v/v) EtOH/H_2O (HEPES buffer, pH 7.4), $\lambda_{ex.}$ 400 nm.

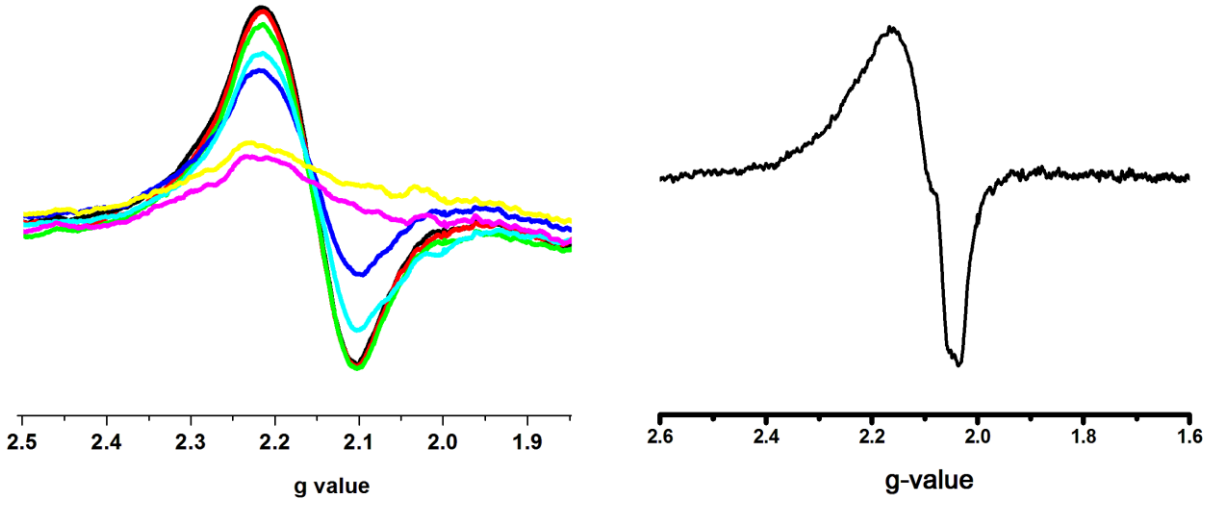

(a) **(b)**

Fig. S20 X- Band EPR spectra (a) gradual addition of [Zn(**L′**)OAc] complex to $CuCl_2$ solution in CH_3CN (b) isolated [Cu(**L′′**)Cl] complex in CH_3CN.

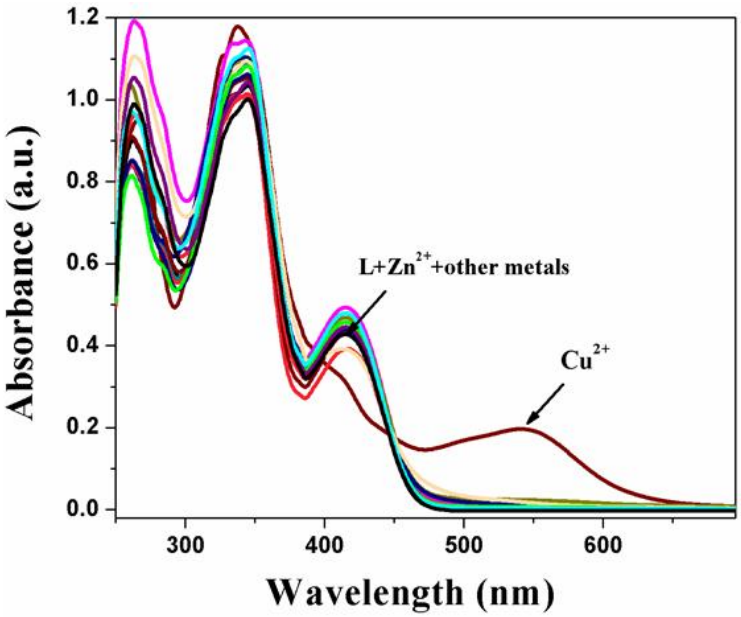

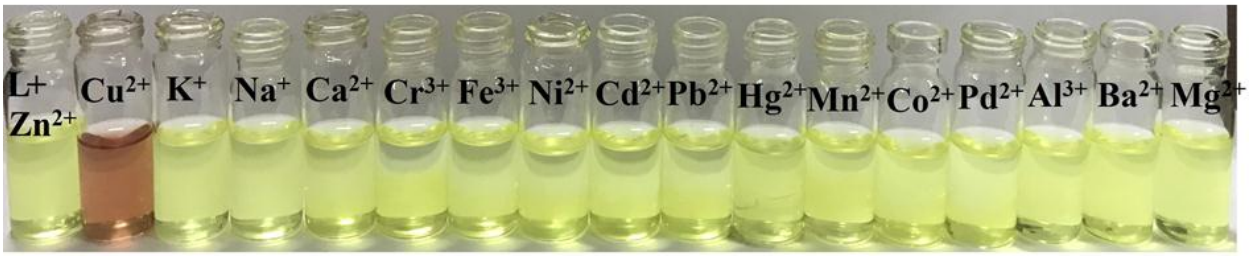

Fig. S21 (a) Absorbance spectra of [Zn(**L′**)OAc]complex in absence and presence of various metal cations in 9:1 (v/v) EtOH/H_2O (HEPES buffer, pH 7.4 (b) vial image in normal light.

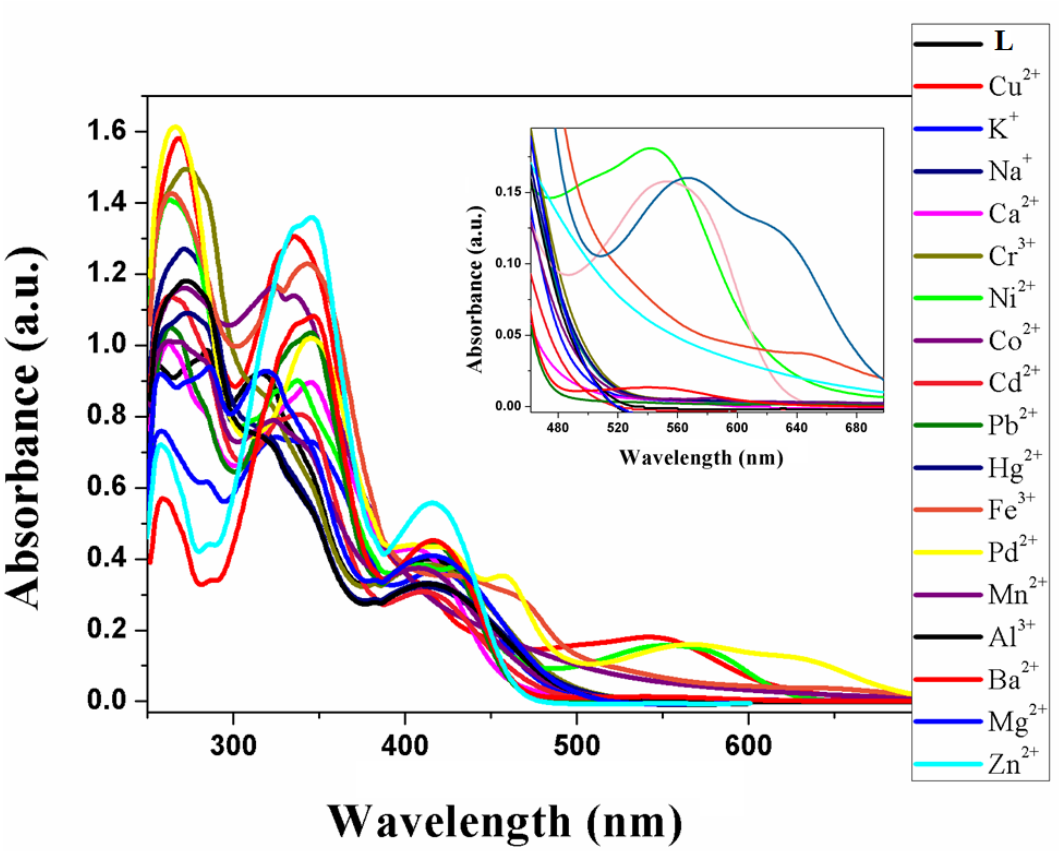

(a)

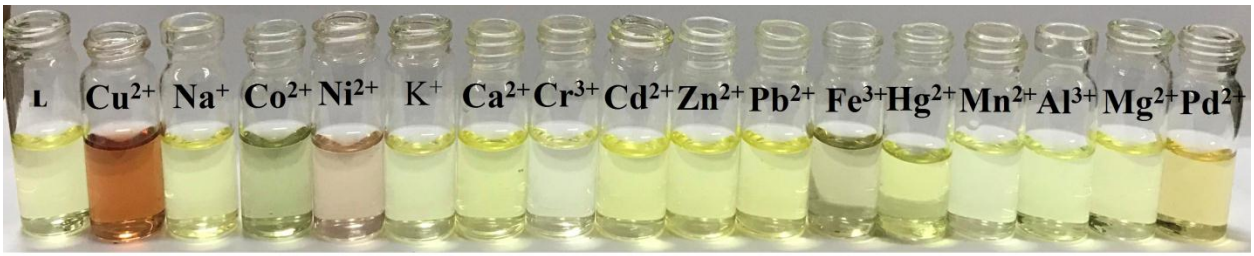

(b)

Fig. S22 (a) Absorbance spectra of ligand, **L** in absence and presence of various metal cations in 9:1 (v/v) EtOH/H_2O (HEPES buffer, pH 7.4; inset: zooming image at higher wavelength. (b) vial image in normal light.

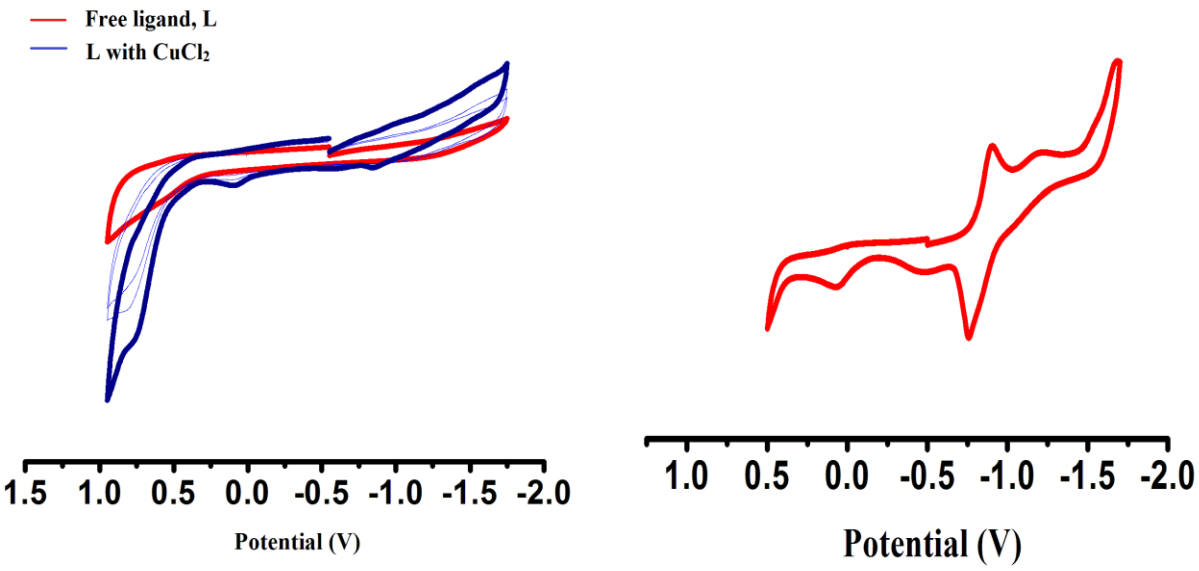

(a) **(b)**

Fig. S23 Cyclic voltammograms (a) **L** and **L** with addition of $CuCl_2$ in CH_3CN in inert atmosphere (b) same solution (**L** and $CuCl_2$ in CH_3CN) kept in air for 10 minutes then pursed with N_2 gas at 296 K, (Conditions: 0.2 M $[N(n\text{-}Bu)_4]PF_6$ supporting electrolyte; scan rate, 100 m V s^{-1}; platinum working electrode).

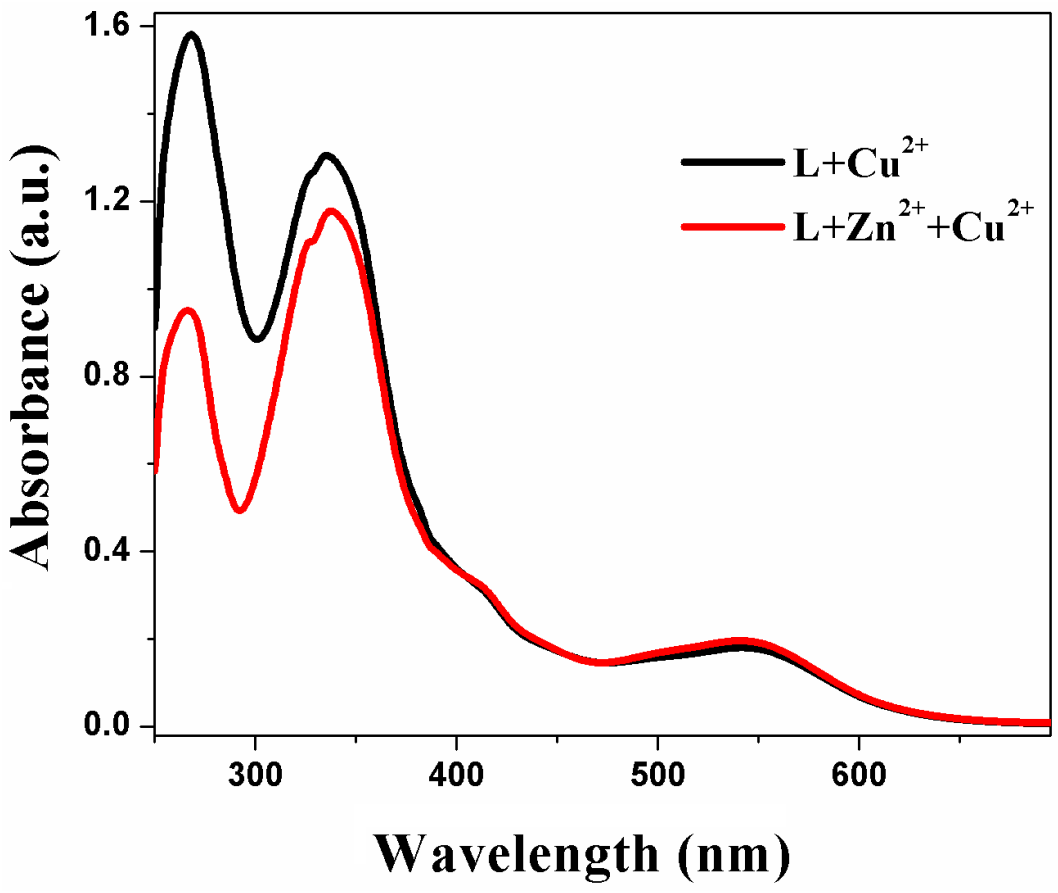

Fig. S24 Absorbance spectra of **L**+Cu^{2+} and **L**+Zn^{2+}+Cu^{2+}.

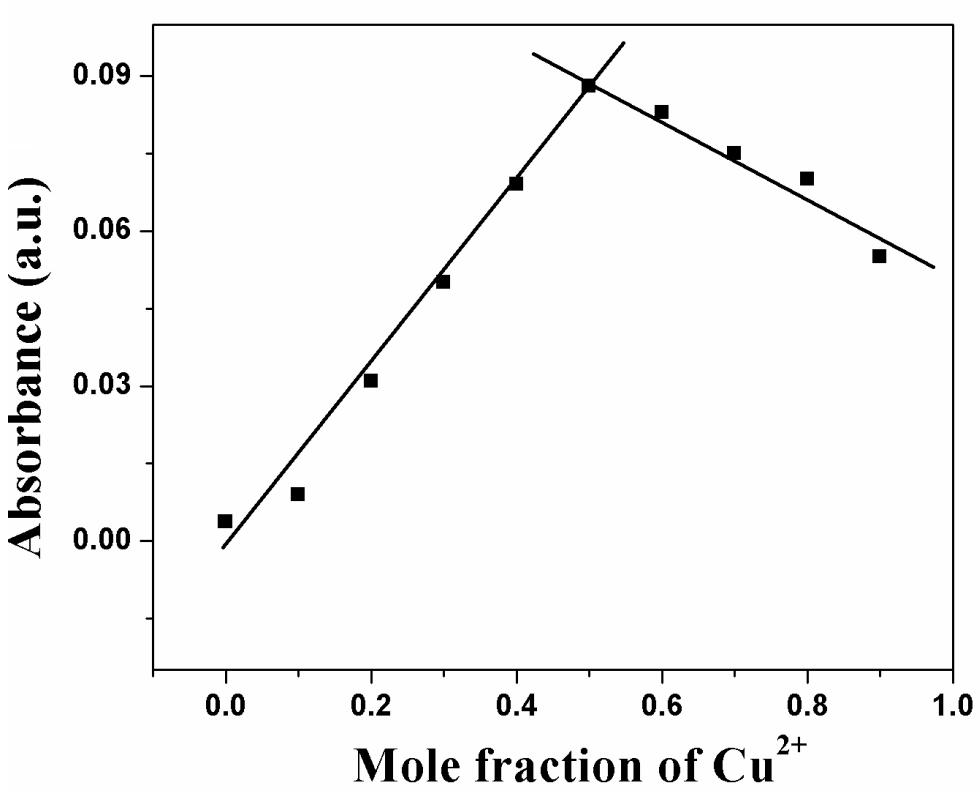

Fig. S25 Job's plot for binding stoichiometry determination for [Zn(L′)OAc] with Cu^{2+} ion.

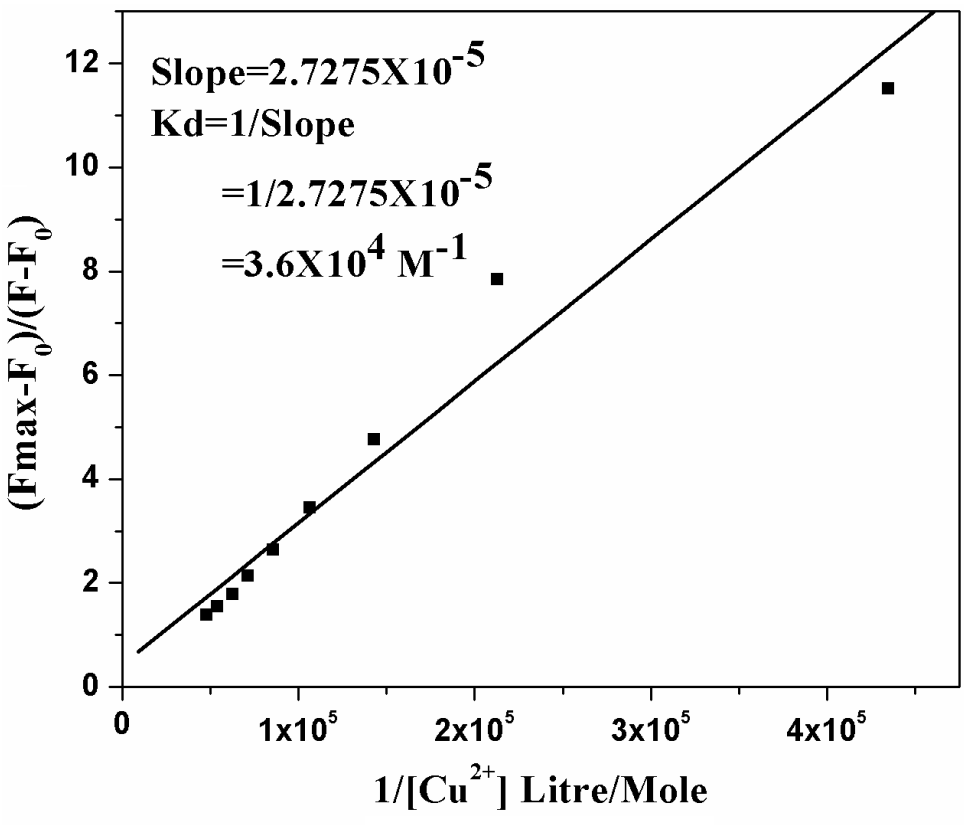

Fig. S26 binding constant for [Cu(**L′′**)Cl] by Benesi-Hildebrand plot.

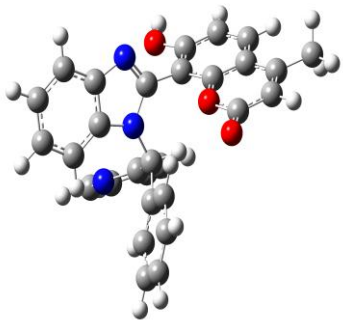	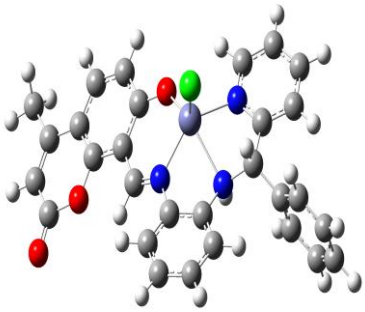	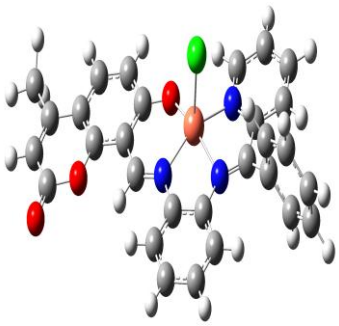
ligand**L**	[Zn(**L′**)]$^{+}$	[Cu(**L′′**)]$^{+}$

Fig. S27 DFT optimized structure of Ligand**L**, [Zn(**L′**)(Cl)] and [Cu(**L′′**)Cl] complex.

Table S6 some frontier molecular orbitals and energies of the ligand **L**

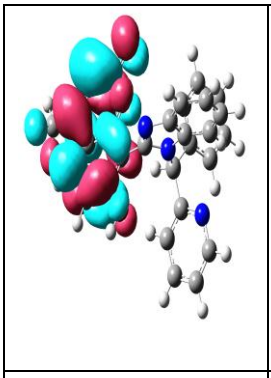	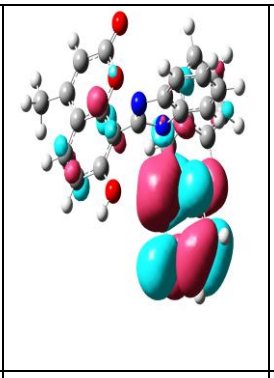	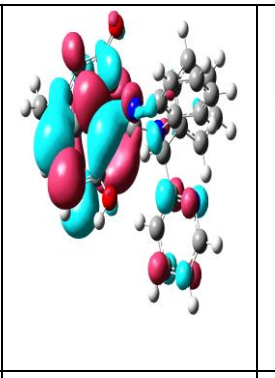	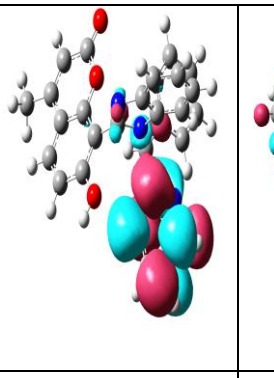	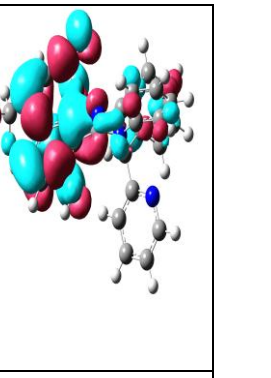
LUMO -2.03eV	LUMO+1 -0.98eV	LUMO+2 -0.75eV	LUMO+3 -0.57eV	LUMO+4 -0.22eV
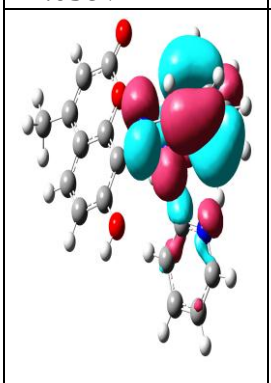	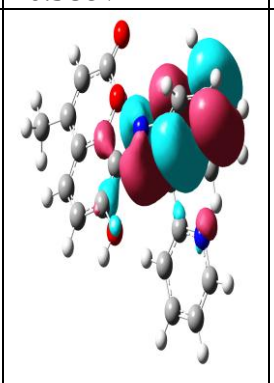	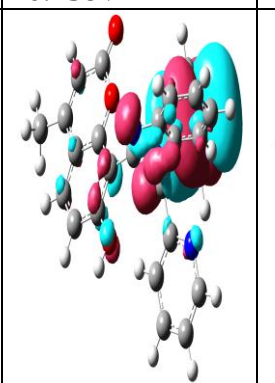	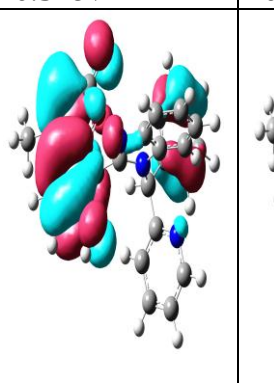	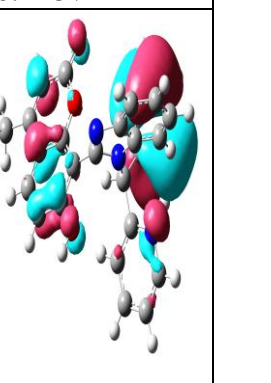
HOMO -5.46 eV	HOMO-1 -5.68 eV	HOMO-2 -6.37 eV	HOMO-3 -6.47 eV	HOMO-4 -6.48 eV

Table S7 some frontier molecular orbitals and energies of the [Zn(**L′**)Cl] complex

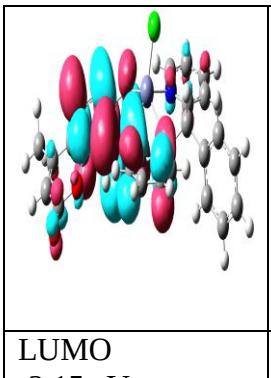	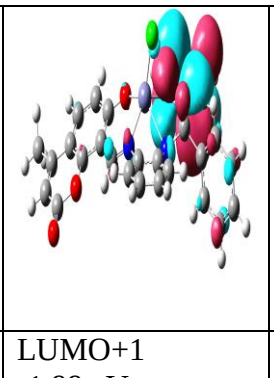	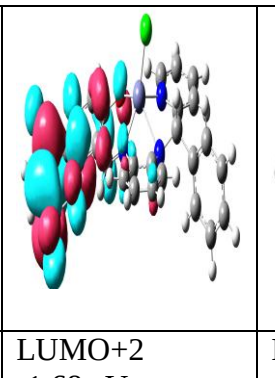	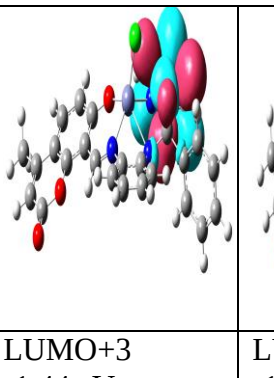	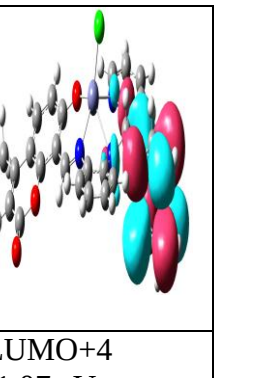
LUMO -2.15 eV	LUMO+1 -1.99 eV	LUMO+2 -1.68 eV	LUMO+3 -1.44 eV	LUMO+4 -1.07 eV

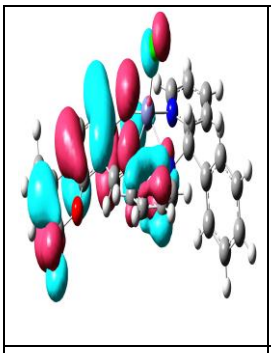	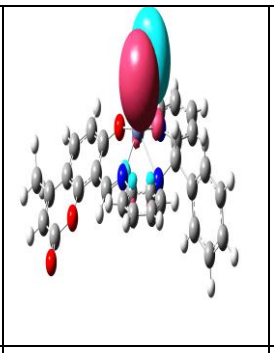	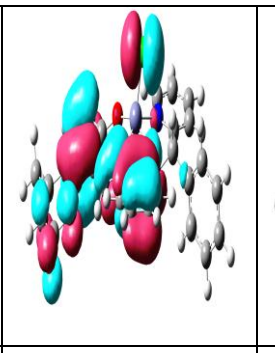	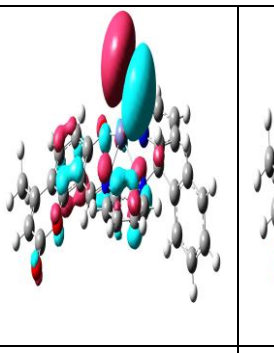	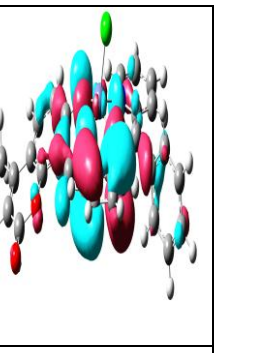
HOMO -5.67 eV	HOMO-1 -6.31 eV	HOMO-2 -6.32 eV	HOMO-3 -6.37 eV	HOMO-4 -6.84 eV

Table S8 some frontier molecular orbitals and energies of the [Cu(**L′′**)Cl] (α spin)

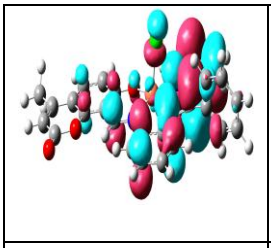	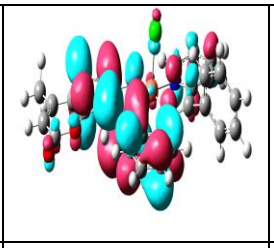	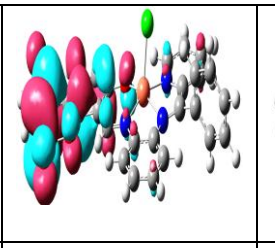	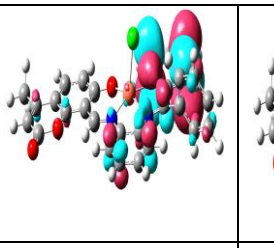	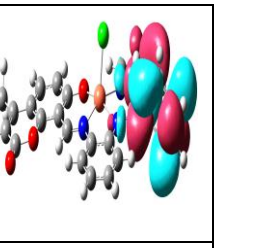
LUMO -3.06 eV	LUMO+1 -2.3 eV	LUMO+2 -1.76 eV	LUMO+3 -1.69 eV	LUMO+4 -1.04 eV
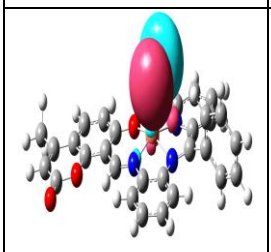	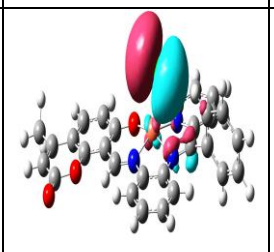	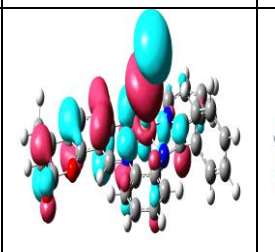	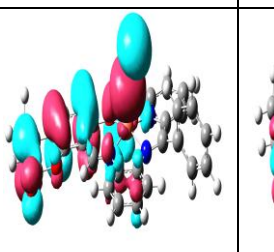	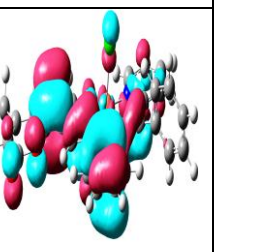
HOMO -5.41 eV	HOMO-1 -5.44 eV	HOMO-2 -5.55 eV	HOMO-3 -5.98 eV	HOMO-4 -6.46 eV

Table S9 Possible electronic transitions on the ligand, **L** from TD-DFT calculation

Excitation energy (eV)	Wavelength Exp. (nm)	Wavelength Thro. (nm)	Oscillation Frequency (f)	Key Transitions	Nature of transition
3.8211 eV	414	324.47	f=0.0087	HOMO-1→LUMO, 47 %	ILCT
4.0784 eV	315	304.01	f=0.3682	HOMO-2→LUMO, 45 %	ILCT

Table S10 Possible electronic transitions on [Zn(**L′**)Cl] complex from TD-DFT calculation

Excitation energy (eV)	Wavelength Exp. (nm)	Wavelength Thro. (nm)	Oscillation Frequency (f)	Key Transitions	Nature of transition
3.1142 eV	414	398.12	f=0.2866	HOMO→LUMO, 43 %	ILCT
3.6763 eV	345	337.26	f=0.6726	HOMO-1→LUMO, 38 %	ILCT (Cl_p→L)

Table S11 Possible electronic transition on [Cu(**L′′**)Cl] complex from TD-DFT calculation

Excitation energy (eV)	Wavelength Exp. (nm)	Wavelength Thro. (nm)	Oscillation Frequency (f)	Key Transitions	Nature of transition
2.3342 eV	540	531.17	f=0.0260	HOMO→LUMO (α), 52 %	ILCT (Cl_p→L)
3.6598 eV	345	338.77	f=0.1501	HOMO-5→LUMO+1 (α), 50 %	ILCT

Table S12 Optimized coordinates for ligand, **L**

Center Number	Atomic Number	Coordinates (Angstroms)		
		X	Y	Z
1	8	5.919369	7.872931	8.041695
2	1	5.833926	8.573460	8.716432
3	8	4.379652	3.586147	6.738146
4	7	6.961271	5.373320	5.655676
5	7	5.171905	6.655104	5.087898
6	8	3.758761	1.525175	6.013425
7	6	5.734815	5.932802	6.043439
8	6	5.120814	5.742444	7.375384
9	6	4.384764	4.590535	7.689995
10	6	5.161365	6.760880	8.341768
11	6	7.186264	5.798379	4.339134
12	6	6.055215	6.587212	4.002090
13	6	8.241316	3.231846	5.818245
14	6	7.828123	4.537721	6.512925
15	1	7.185014	4.256406	7.354498

16	6	3.681122	4.430561	8.906247
17	6	8.969542	5.358718	7.101463
18	6	2.931678	3.201472	9.120302
19	6	4.475745	6.635809	9.564251
20	1	4.519648	7.439984	10.292634
21	6	3.742791	5.489124	9.835203
22	1	3.213534	5.408175	10.777141
23	7	9.862926	5.899500	6.240996
24	6	5.941471	7.168107	2.732064
25	1	5.072108	7.767390	2.486445
26	6	8.226700	5.580592	3.426262
27	1	9.103841	5.009744	3.695494
28	6	9.562891	2.761601	5.823370
29	1	10.351737	3.358394	6.263833
30	6	3.670452	2.354887	6.916435
31	6	7.238873	2.441462	5.227077
32	1	6.210818	2.785050	5.222009
33	6	6.969045	6.946387	1.819054
34	1	6.911161	7.380909	0.826043
35	6	8.095120	6.163760	2.166255
36	1	8.882065	6.015525	1.433270
37	6	2.938865	2.233897	8.158097
38	1	2.392081	1.308202	8.285079
39	6	9.878565	1.527201	5.240370
40	1	10.907417	1.180266	5.246529
41	6	9.066257	5.558900	8.485835
42	1	8.336081	5.111531	9.152018
43	6	2.154641	3.009024	10.397605
44	1	1.648046	2.041255	10.403801
45	1	1.395039	3.790815	10.521279
46	1	2.812695	3.053439	11.274364
47	6	7.555862	1.210240	4.648303
48	1	6.766035	0.614178	4.203121
49	6	11.023750	6.910043	8.101162
50	1	11.843202	7.527168	8.452255
51	6	8.878205	0.748107	4.652077
52	1	9.124416	-0.208551	4.201750
53	6	10.108860	6.341627	8.992516
54	1	10.202705	6.505993	10.061060
55	6	10.860378	6.662130	6.734222
56	1	11.545058	7.079421	6.003359

Table S13 Optimized coordinates for [Zn(**L′**)Cl] complex

Center Number	Atomic Number	Coordinates (Angstroms)		
		X	Y	Z
1	8	14.488700	3.145237	13.809071
2	7	14.333733	1.827862	11.263424
3	7	16.693662	0.609007	11.596967
4	1	17.113682	1.505973	11.345774
5	6	17.978751	0.566161	13.667558
6	6	13.557499	2.851793	10.974551
7	1	13.170731	2.968854	9.960496
8	6	13.163360	3.891074	11.899367
9	6	18.843746	-0.777808	11.676699
10	6	15.848805	0.086720	10.544568
11	6	12.264024	4.893014	11.424450
12	6	14.632878	0.796671	10.324574
13	6	13.636413	3.994123	13.268204
14	6	17.604958	-0.242155	12.402484
15	1	16.996101	-1.091893	12.745060
16	6	11.802312	5.965494	12.215071
17	7	17.052308	1.461284	14.109186
18	6	16.156918	-1.034711	9.757535
19	1	17.081629	-1.576899	9.919861
20	6	12.282696	6.034105	13.560315
21	1	11.945377	6.844064	14.201038
22	6	13.162370	5.095818	14.064946
23	1	13.522263	5.148397	15.087636
24	6	19.168524	-2.146881	11.763731
25	1	18.523490	-2.816099	12.330716
26	6	19.685773	0.077088	10.933093
27	1	19.456099	1.138626	10.854393
28	6	15.272020	-1.448944	8.744549
29	1	15.513600	-2.321480	8.143336
30	6	10.877174	6.921588	11.631233
31	6	13.759664	0.379673	9.298395
32	1	12.812008	0.889967	9.150406
33	6	10.932235	5.689906	9.474625
34	6	19.179458	0.374465	14.374489
35	1	19.911872	-0.339891	14.017030
36	6	10.474636	6.772873	10.322828
37	1	9.785183	7.468194	9.857531
38	6	21.142350	-1.799260	10.374177
39	1	22.022359	-2.190545	9.869812

40	6	14.082249	-0.735149	8.507368
41	1	13.397964	-1.057755	7.727266
42	6	20.824794	-0.428941	10.282812
43	1	21.461530	0.238511	9.707186
44	6	20.311373	-2.657686	11.118259
45	1	20.546885	-3.716504	11.191489
46	6	18.450628	2.049151	15.980476
47	1	18.600455	2.642810	16.876222
48	6	19.412636	1.119191	15.544900
49	1	20.332570	0.976547	16.105477
50	6	17.274489	2.193348	15.229012
51	1	16.484645	2.885888	15.502621
52	8	10.641981	5.465030	8.292671
53	8	11.842021	4.763554	10.105614
54	6	10.357422	8.074585	12.461679
55	1	9.817554	7.711694	13.346477
56	1	11.180003	8.708822	12.818449
57	1	9.674061	8.699696	11.879457
58	30	15.127998	1.365323	13.162557
59	17	14.356592	-0.666807	14.027198

Table S14 Optimized coordinates for [Cu(**L″**)Cl] complex

Center Number	Atomic Number	Coordinates (Angstroms)		
		X	Y	Z
1	29	11.770658	4.214216	13.010733
2	8	7.253934	1.528512	11.473454
3	8	11.903742	2.826455	11.638165
4	8	5.041835	0.956576	11.486971
5	7	9.905570	3.787892	13.471032
6	7	13.751763	4.460161	13.260979
7	7	11.763850	5.115884	14.838742
8	6	9.132619	2.987793	12.764727
9	1	8.089853	2.852212	13.046557
10	6	9.460032	4.500048	14.621836
11	6	9.536998	2.227817	11.613385
12	6	10.457119	5.215647	15.362242
13	6	10.893865	2.169840	11.105148
14	6	14.045453	5.309218	14.294269
15	6	8.536884	1.452209	10.947686
16	6	13.043289	6.893480	16.051583
17	6	8.798457	0.647194	9.822686
18	6	6.130004	0.809777	10.917191

19	6	12.884347	5.727182	15.127948
20	6	8.117657	4.541445	15.056708
21	1	7.337666	4.038497	14.494832
22	6	8.755449	5.915220	16.969097
23	1	8.483275	6.450220	17.874688
24	6	10.088719	5.906131	16.540930
25	1	10.838035	6.431682	17.118456
26	6	10.148575	0.613379	9.347853
27	1	10.387184	0.005173	8.479955
28	6	11.153604	1.334410	9.961427
29	1	12.175107	1.307937	9.596166
30	6	7.702103	-0.088916	9.215957
31	6	14.709861	4.031369	12.417373
32	1	14.375659	3.378047	11.617923
33	6	6.437249	0.003196	9.752491
34	1	5.597867	-0.532434	9.323656
35	6	13.647963	6.777059	17.320615
36	1	13.993238	5.806748	17.671670
37	6	7.768516	5.242023	16.219140
38	1	6.730358	5.263911	16.539720
39	6	12.590054	8.153812	15.595921
40	1	12.134121	8.229685	14.610499
41	6	16.049439	4.434387	12.570797
42	1	16.804782	4.077036	11.878741
43	6	15.363312	5.761566	14.490504
44	1	15.585410	6.454156	15.294233
45	6	13.785137	7.912975	18.141484
46	1	14.242977	7.818583	19.123016
47	6	16.374126	5.312887	13.620740
48	1	17.397474	5.651616	13.756401
49	6	7.953173	-0.951555	7.998886
50	1	7.031334	-1.437692	7.666508
51	1	8.693047	-1.734222	8.213738
52	1	8.343240	-0.353377	7.164583
53	6	12.736680	9.285288	16.417798
54	1	12.389321	10.253011	16.065256
55	6	13.330482	9.167938	17.691056
56	1	13.438949	10.044968	18.324466
57	17	11.481686	6.484428	12.022982

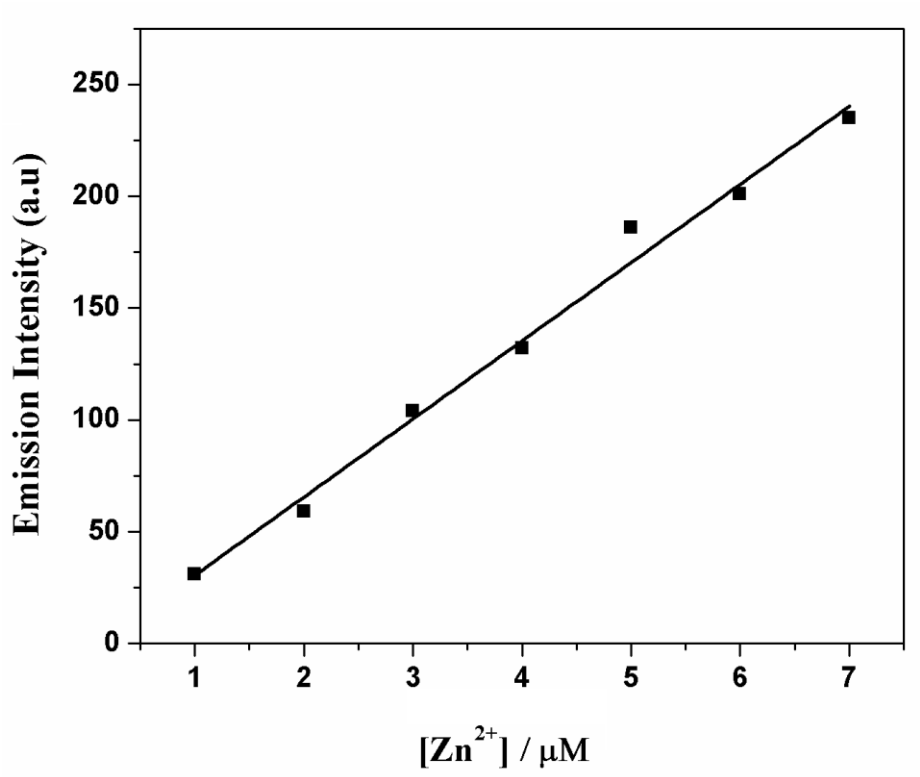

Fig. S28 Calibration plot for recovery of Zn^{2+} ion.

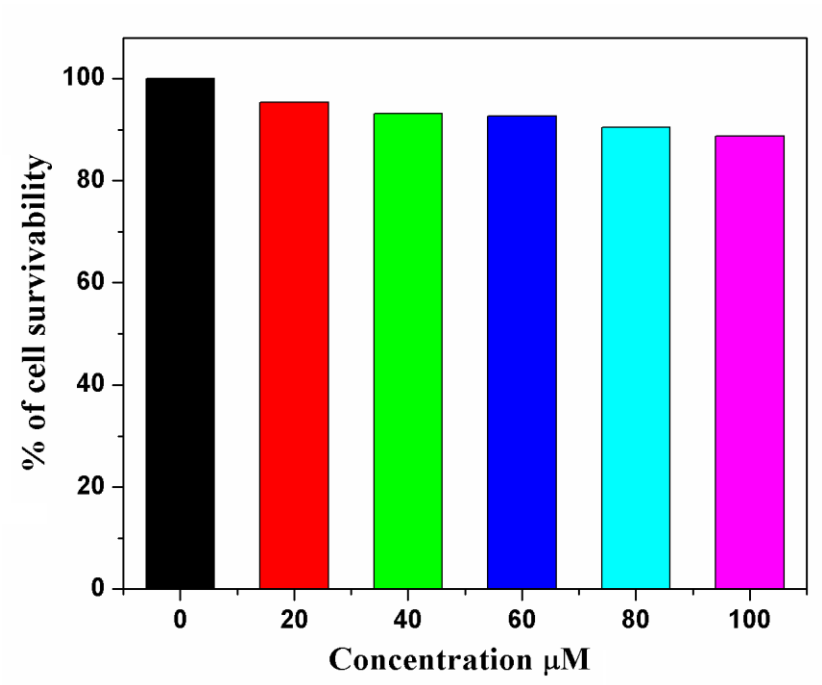

Fig. S29 Cell survivability of WI-38 cells exposed to **L**.

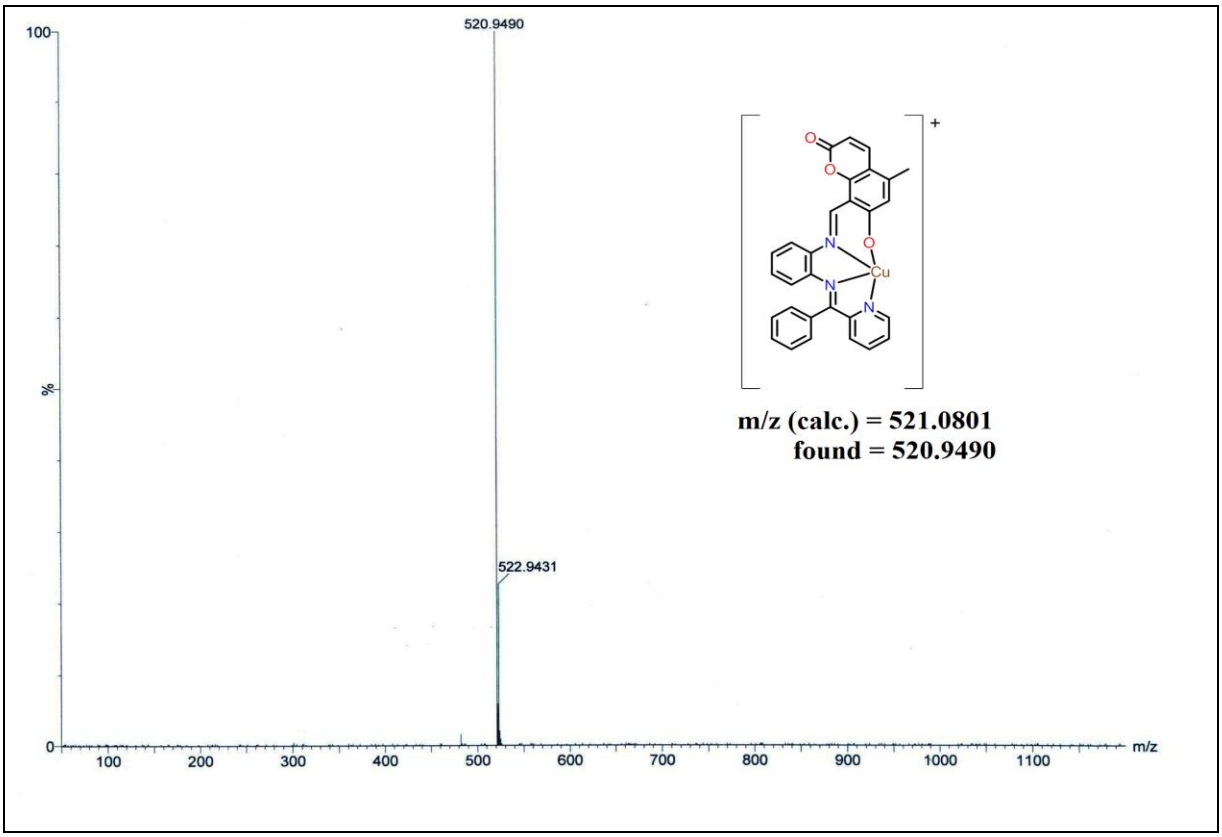

Fig. S30 ESI-MS spectrum of [Cu(**L′′**)Cl] complex.

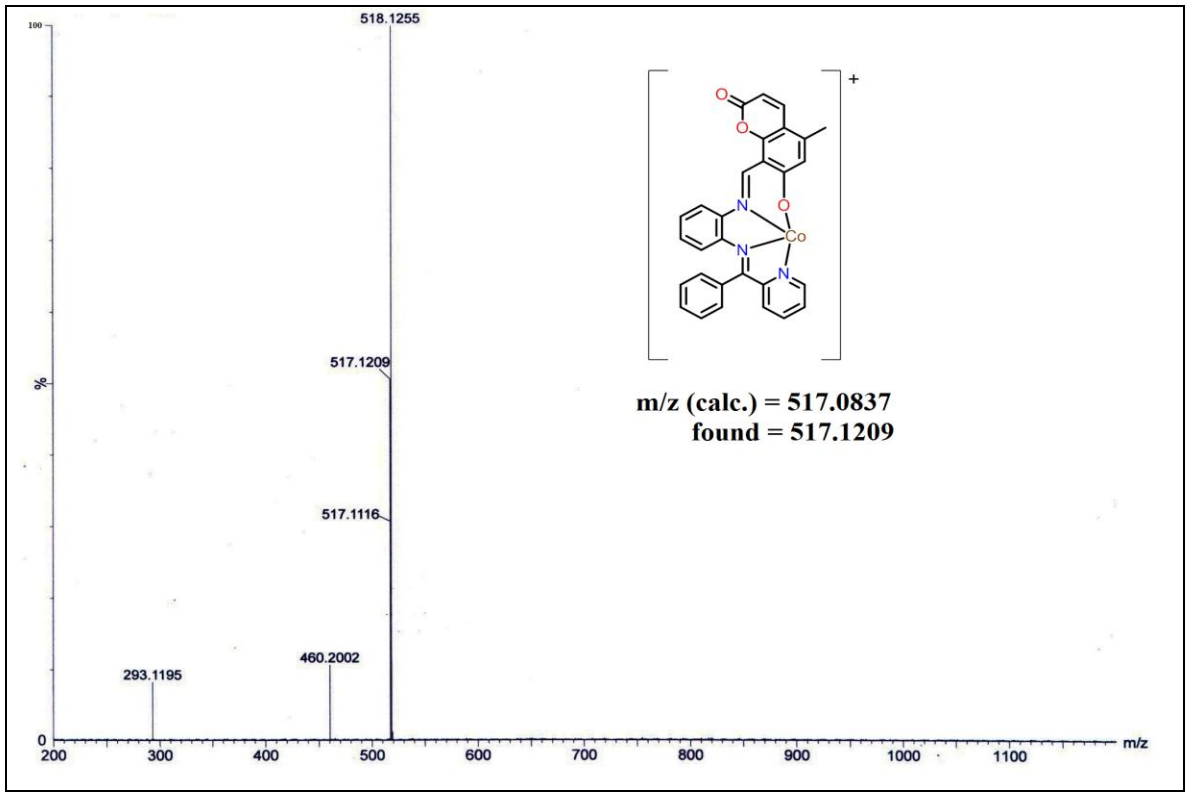

Fig. S31 ESI-MS spectrum of [Co(**L''**)(NO_3)] complex.

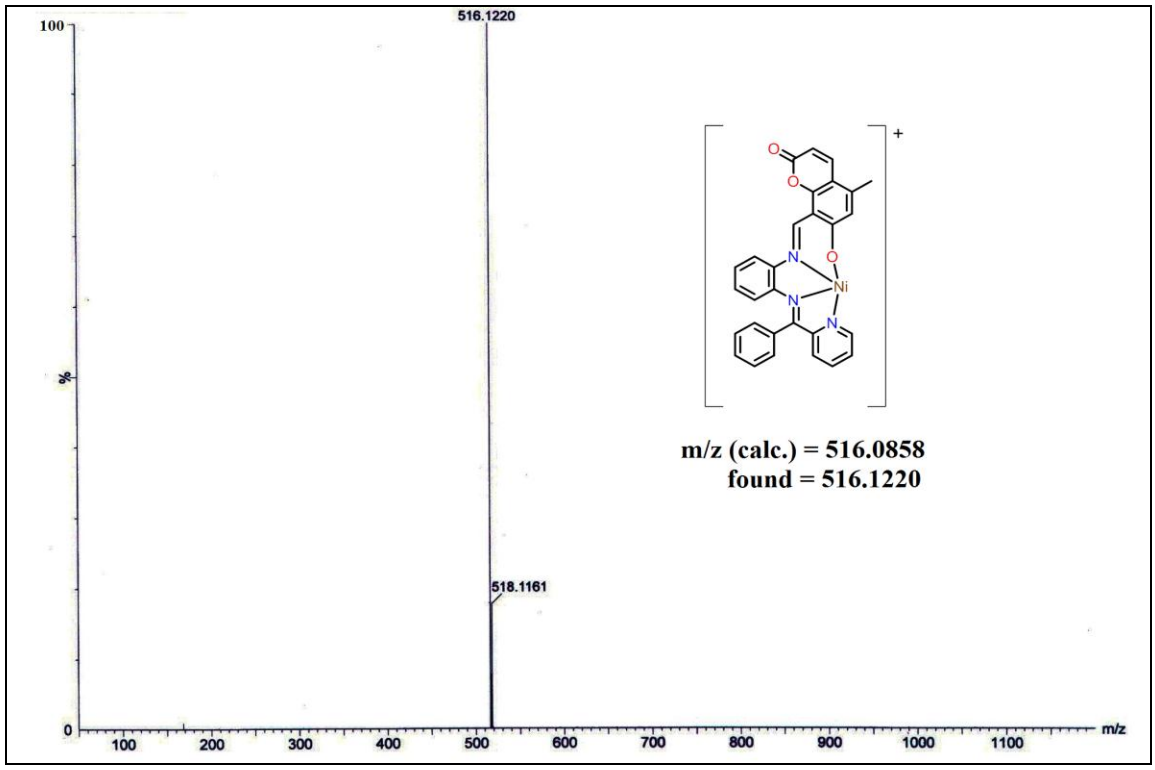

Fig. S32 ESI-MS spectrum of [Ni(**L''**)(Cl)] complex.

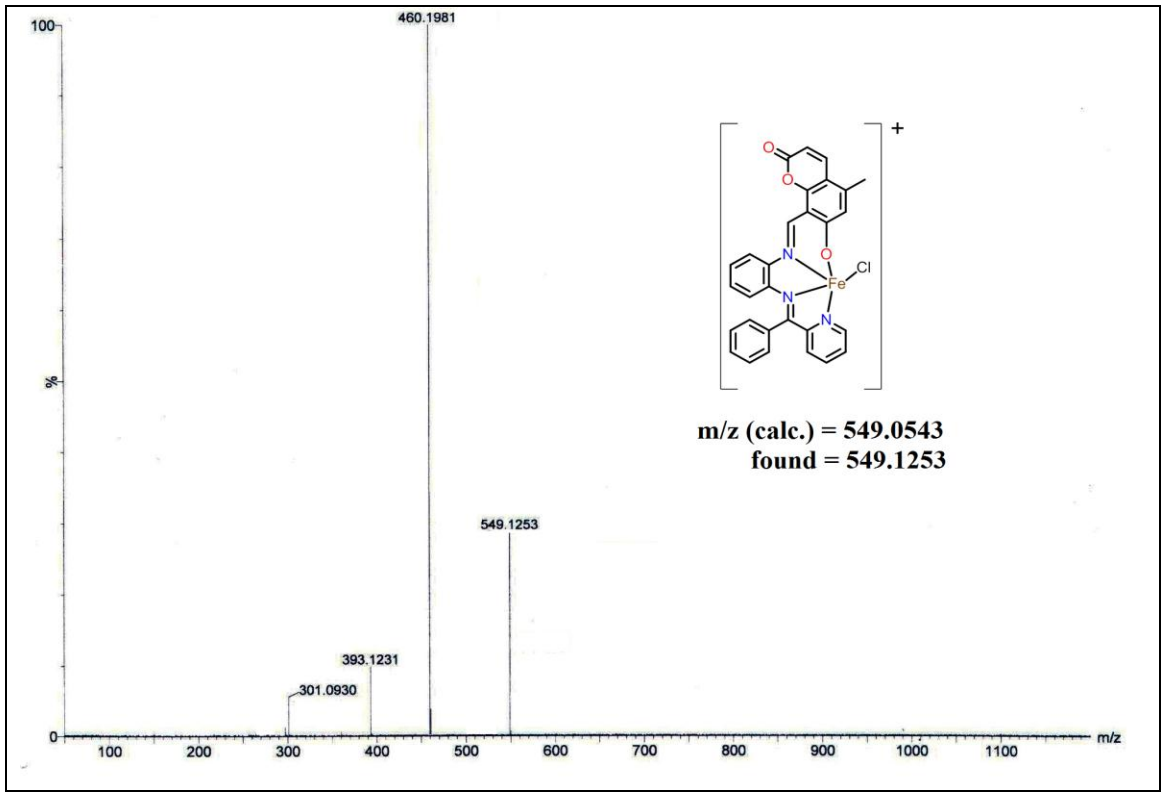

Fig. S33 ESI-MS spectrum of [Fe(**L''**)(Cl)$_2$] complex.

References

1 S. Chaudhuri, S. C. Patra, P. Saha, A. S. Roy, S. Maity, S. Bera, P. S. Sardar, S. Ghosh, T. Weyhermüllerc and P. Ghosh, *Dalton Trans.*, 2013, **42**, 15028-15042.

2 K. Das, U. Panda, A. Datta, S. Roy, S. Mondal, C. Massera, T. Askun, P. Celikboyun, E. Garribba, C. Sinha, K. Anand, T. Akitsu and K. Kobayashi, *New J. Chem.*, 2015, **39**, 7309-7321.

3 D. D. Perrin, W. L. F. Armarego, D. R. Perrin, Purification of Laboratory Chemicals, Pergamon Press, Oxford, U.K., 1980.

4 D. Maiti, A. S. M. Islam, M. Sasmal, C. Prodhan and Mahammad Ali, *Photochem. Photobiol.Sci.*, 2018, **17**, 1213-1221.

5 A. Samui, K. Pal, P. Karmakar and S. K. Sahu, *Mater. Sci. Eng.* C, 2019, **98**, 772-781.

6 K. Pal, S. Roy, P. K. Parida, A. Dutta, S. Bardhan, S. Das, K. Jana and P. Karmakar, *Mater. Sci. Eng.* C, 2019, **95**, 204-216.

7 Y. Gao, H. Liu, P. Li, Q. Liu, W. Wang and B. Zhao, *Tetrahedron Letters* 2017, **58**, 2193-2198.

8 M. Yan, T. Li and Z. Yang, *Inorg. Chem. Comm.*, 2011, **14**, 463-465.

9 J.-H. Hu, Y. Suna, J. Qi, Q. Li and T.-B. Wei, *Spectrochim. Acta, Part* A, 2017, **175**, 125-133.

10 C. Patra, A. K. Bhanja, A. Mahapatra, S. Mishra, K. D. Saha, C. Sinha, *RSC Adv.*, 2016, **6**,76505-76513.

11 C. Patra, C. Sen, A.D. Mahapatra, D. Chattopadhyay, A. Mahapatra and C. Sinha, *J. Photoch. Photobio.* A, 2017, **341**, 97-107.

12 S. Dey, R. Purkait, C. Patra, M. Saha, S. Mondal, K. D. Saha and Chittaranjan Sinha, *New J. Chem.*, 2018, **42**, 16297-16306.

13 D. Sarkar, A. K. Pramanik and T. K. Mondal, *J. Lumin.*, 2014, **146**, 480-485.

14 J.-m. An, M.-h. Yan, Z.-y. Yang, T.-r. Li and Q.-x. Zhou, *Dyes Pigm.*, 2013, **99**, 1-5.

15 M. Z. Jonaghani, H. Zali-Boeini and H. Moradi, *Spectrochim. Acta, Part* A, 2019, **207**, 16-22.

16 D. Sarkar, A. K. Pramanik and T. K. Mondal, *RSC Adv.*, 2015, **5**, 7647-7653.

17 M. L. Aulsebrook, B. Graham, M. R. Grace and K. L. Tuck, *Supramol. Chem.*, 2015, **27**, 798-806.